AFIT/GNE/ENP/93M-03

AD-A262 612

ANALYSIS OF TOPAZ II AND SPACE-R SPACE
NUCLEAR POWER PLANTS USING A
MODIFIED THERMIONIC MODEL

THESIS

Otto D. Habedank, First Lieutenant, USAF
AFIT/GNE/ENP/93M-03

DTIC
S ELECTE
E APR 05 1993 **D**

93-06891

98 ' 4 02 050

Approved for public release; distribution unlimited.

20001006131

AFIT/GNE/ENP/93M-03

ANALYSIS OF TOPAZ II AND SPACE-R

SPACE NUCLEAR POWER PLANTS

USING A MODIFIED THERMIONIC MODEL

THESIS

Presented to the Faculty of the School of Engineering

of the Air Force Institute Of Technology

Air University

In Partial Fulfillment of the

Requirements for the Degree of

Master of Science in Nuclear Engineering

Otto D. Habedank, B.S.

First Lieutenant, USAF

March 1993

DTIC QUALITY INSPECTED 4

Approved for public release; distribution unlimited

Preface

The purpose of this study was to use TDS, a thermionic diode model developed by Phillips Laboratory, to conduct parameter studies on the TOPAZ II and SPACE-R space nuclear power systems. TOPAZ II and SPACE-R nuclear core designs are based on single-cell thermionic fuel cells. The model was written to run in a modeling environment developed by Argonne National Laboratory called General Purpose Simulation Language (GPS).

The SPACE-R model developed was unable to converge on a solution due to TDS's inability to evaluate the complex electrical geometry of the design. TDS was successful in converging on solutions for TOPAZ II. Four parameter studies of TOPAZ II were conducted to demonstrate the utility of GPS and to provide data requested by the sponsors at Phillips Lab. The complete results of this thesis also include the modifications and the system modeling approach developed for the unsuccessful SPACE-R model. With this work out of the way, follow up testing of the SPACE-R system should be more easily accomplished to test the utility of the design. Furthermore, the model is becoming considerably more flexible than originally designed, allowing different thermionic fuel element arrangements to be studied.

To complete this thesis required interaction with both Ralph Peters, primary author of TDS, and Howard Geyer, primary author of GPS. This interaction was necessary as both codes are still in the developmental stage and my problem required further modification of both. I am indebted to both of them for working diligently with me on this project. Overseeing them and also helping greatly with the project were Captain Mark Dibben at Phillips Laboratory and Tom Ewing at Argonne National Laboratory. Thanks also goes to the Space Power Division at Phillips Laboratory for sponsoring my project. Closer to home, thanks goes out to my faculty advisor, Lt. Col. Denis Beller, who assisted me and constantly reminded me of the final goal, this report.

TABLE OF CONTENTS

iv

LIST OF FIGURES

LIST OF TABLES

vii

Abstract

Models based on the TDS thermionic diode model were developed for the TOPAZ II and SPACE-R nuclear power systems. Due to computer code limitations inherent in the TDS model, only the TOPAZ II system model ran successfully. Several parameter studies were conducted on the TOPAZ II model. These studies determined system performance and efficiency while varying the following:

       1. The coolant flow inlet temperatures.

       2. The rate of coolant temperature change.

       3. The power profile of the core.

       4. The cesium reservoir temperature.

Analysis of the results indicate that the model accurately represented the TOPAZ II system, underestimating published data by 10%. Coolant flow parameter studies indicate that raising coolant flow temperatures up to 100 K higher increases system power by up to 5%. Additional increases in temperature result in gradual performance degradation. Varying the axial power profile of the core from the actual peaked profile to a flat profile results in a negligible 0.3% change in total system performance. The peaked profile used in TOPAZ II produces the highest system efficiency of all the profiles modeled. The cesium pressure study indicates that the system is operating above optimum cesium pressure and that system performance is strongly dependent on cesium pressure. Increasing cesium reservoir temperature above design temperature by 30 K decreases system efficiency by 30%.

ANALYSIS OF TOPAZ II AND SPACE-R SPACE NUCLEAR POWER PLANTS USING A MODIFIED THERMIONIC MODEL

I. Introduction

The United States, through the Space Exploration Initiative, has committed itself to expanding its knowledge of the universe and to establishing a permanently manned presence in space. Additionally, the United States Air Force and the Strategic Defense Initiative Organization (SDIO) have a definite interest in maintaining a presence in space. To accomplish the goals of both exploration and defense; compact, light weight power sources are required. These power requirements often can best be met through the use of space nuclear power systems. One of the primary facets in this arena is the development of thermionic power systems. The unique advantages offered by thermionic power systems include modularity, high waste heat rejection temperatures, and the stable electrical characterist.cs of the thermionic conversion process.(13:617)

Even though nuclear thermionic devices have been developed and used in space for years, many aspects of their operation are still a mystery. A definite need exists to develop models which can help determine thermionic system characteristics so that they can be optimized for space applications.

To help understand and develop thermionic space systems the United States purchased the TOPAZ II space nuclear power system from the Former Soviet Union. It utilizes a core of thermionic fuel elements (TFE) which are made up of a uranium center surrounded by a thermionic converter. The utilization of TFE's allows for flexibility in core modifications. Depending on the number of TFE's used and the method in which

1

they are electrically connected, numerous nuclear systems can be configured to fit varied power requirements.

The United States Air Force's Phillips Laboratory and Argonne National Laboratory are working together to develop a model, the Thermionic Diode Subsystem Model (TDS), which can be used to model different types of TFE's and different system configurations. At present the model is only being used to model the TOPAZ II system, but it is being developed in a manner which allows for follow on applications in the modeling of new power systems which utilize the TFE core concept.

This study utilized TDS to conduct parameter studies of TOPAZ II. The failed attempt to use TDS to model a larger 40 kW_e space nuclear power system proposed by Space Power Incorporated (SPI) entitled Space Power Advanced Core-length Element Reactor (SPACE-R) is found in Appendix A. The parameter studies conducted on TOPAZ II dealt with the effects of changing:

   1. The coolant flow inlet temperatures.

   2. The rate of coolant temperature change.

   3. The power profile of the core.

   4. The cesium reservoir temperature.

II. Background

Thermionic Converter Theory

    Thermionic conversion is a method for converting heat directly into an electric current through the use of a phenomenon called thermionic emission. The principal device for producing thermionic conversion is called a thermionic converter. In its most basic form, it consists of an electrode called the emitter, that is connected to a heat source and a second electrode, called the collector, that is connected to a heat sink and is separated from the first by an intervening space. Leads connect the electrodes to the electrical load. A simple schematic of it is shown in Figure 1. Electrons move through the intervening space from the emitter to the electrode where they collect and return to the hot emitter via the electrical leads and the electrical load. The flow of electrons through the electrical load is sustained by the temperature differential. A thermionic converter in essence is a heat engine since it receives heat at high temperature, rejects it at low temperature, and produces electrical work while it is operating. (11: 1-3)

3
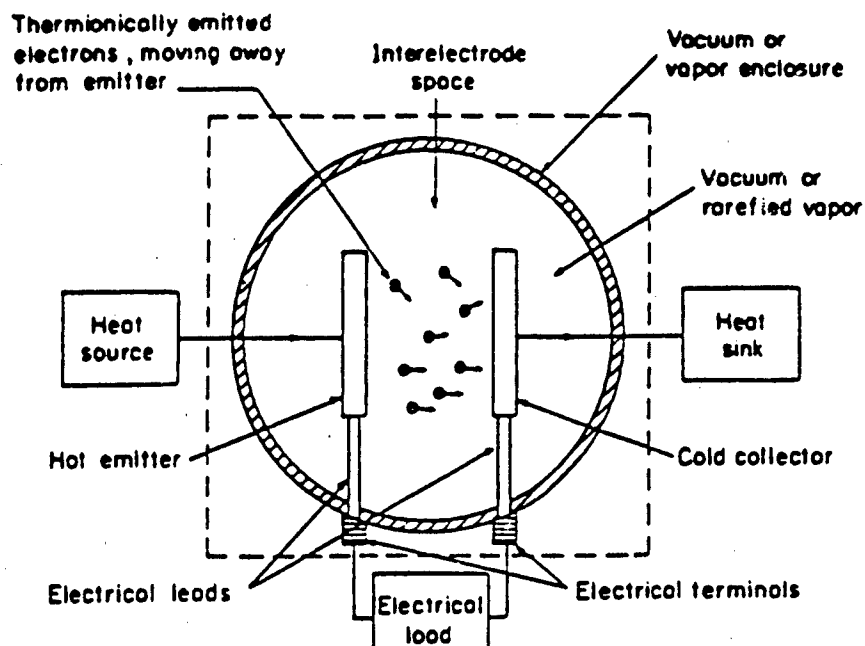
Figure 1. Simple Thermionic Diode (11)

The physics of how thermionic converters provide an electric current is illustrated in a potential diagram of the system. Such a diagram of an ideal thermionic diode is shown in Figure 2, where V load is the load voltage of the system and V drop is the voltage drop between the cathode and anode which accelerates electrons released from the cathode across the interelectrode gap to the anode.

4
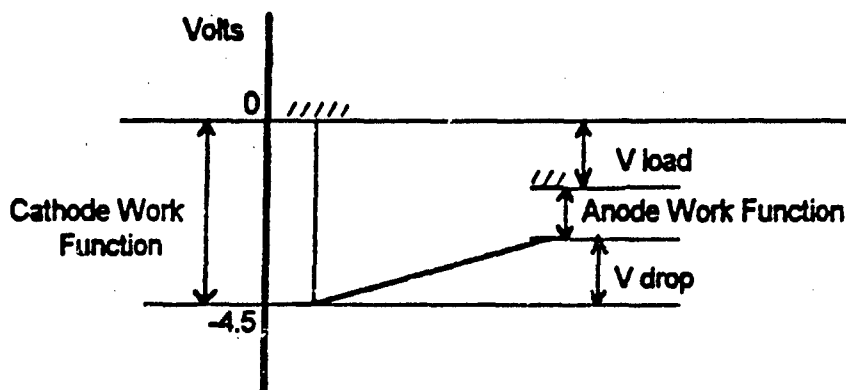
Figure 2. Potential Diagram of an Ideal Diode (14)

Both surfaces emit thermionic electrons according to the Richardson-Dushmann
equation:

$$J_s = AT^2 \exp\left(-\frac{\phi}{kT}\right) \tag{1}$$

where ϕ in this case is the effective work function that the electrons have to overcome, A
is Richardson's constant and equals 120 A/cm^2-K^2, T is the temperature of the emitting
surface in kelvin, and k is Boltzmann's constant and equals 1/11600 eV/K. In a thermionic
converter the collector emission current is virtually negligible due to large temperature

differences between the emitter and collector. The emitted electrons from the emitter enter the inter-electrode gap where they are accelerated by the electric field and flow to the collector. As long as the emitter work function is greater than the sum of the collector work function and the load voltage, an accelerating electric field will exist and current will flow through the circuit. The accelerating field also has a positive effect on the rate of emission. This increase in emission due to moderately strong external fields is called the Schottky effect. (11:38)

The inter-electrode space of a thermionic converter is usually filled with a rarefied vapor. The vapor is introduced to negate the negative space-charge effect which occurs if no gas is present. The space charge occurs because of the amount of electrons present in the gap at any given time. These electrons produce an electric field which opposes the accelerating field, thus reducing the amount of emission as the Schottky effect is reduced. The space charge is neutralized by positive gas ions which are produced when the vapor is ionized. The vapor most commonly used is cesium since it is the most easily ionized of the stable gases. The ionization occurs when the cesium atoms are adsorbed on the emitter surface. They then are thermionically emitted as positive cesium ions. Another mode of ionization occurs in the gap through inelastic collisions between vapor atoms and emitted electrons. The ionized cesium gas forms a plasma between the emitter and collector, canceling out space-charge effects. (11:7)

Another effect of vapor ionization depends on how the ionization occurs. When the primary mode of ionization is thermionic emission from the emitter surface the converter is said to be operating in the unignited or diffusion mode. When the primary mode of ionization is due to inelastic collisions in the interelectrode gap, the converter is operating in the ignited mode. The ignited mode is characterized by a jump in converter efficiency due to the fact that the inelastic collisions not only create positive ions which negate space-charge effects, but they also liberate electrons which contribute to the current. The

6

ignited mode can further be separated into the obstructed and the saturated regions. In the obstructed region the space-charge effects are not completely negated by the positive ion plasma, whereas the saturated region is characterized by a positive electric field existing at the emitter surface which accelerates virtually all the emitted electrons into the plasma.(14:6)

Current density vs. voltage plots (J-V curves) are often used to show how a thermionic diode is operating. Each J-V curve represents a thermionic diode operating with fixed Cesium pressure, collector temperature, and emitter temperature. Changing any of the fixed variables causes the shape and position of the J-V curve to change. A J-V curve which outlines the different regions and modes is shown in Figure 3. In it J_{ES} represents the current density saturation line for the ideal diode, J_D and V_D represent the differences in actual thermionic diode current densities and voltage compared to the ideal diode, J_{PS} represents the current density saturation line if the diode is operating in the unignited mode, and J_{RS} is the reverse current saturation density which occurs when a large voltage load is applied. (11:177)
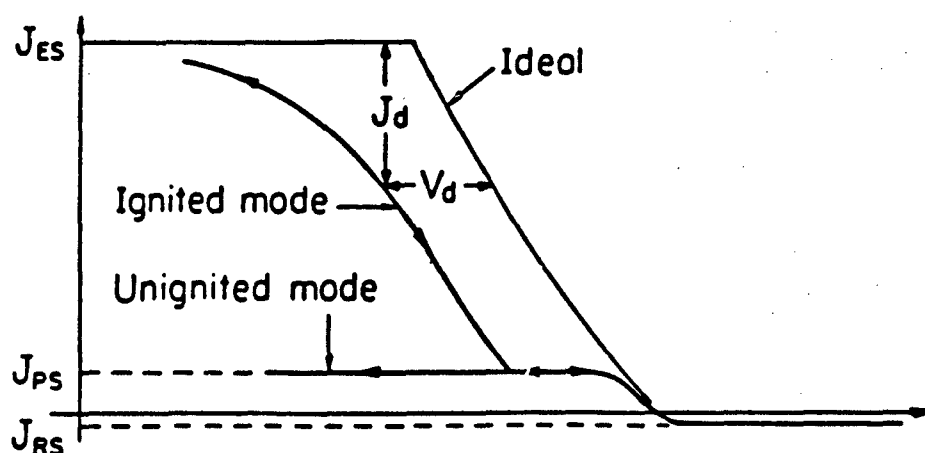
Figure 3. J-V Curves for Different Modes of a Thermionic Converter(11)

A family of J-V curves with changing collector temperatures is shown in Figure 4. It represents actual measurements made on a tungsten thermionic converter. In it T_E is the emitter temperature, T_C is the collector temperature, T_R is the cesium reservoir temperature, and d is the interelectrode gap. A family of J-V curves with changing cesium reservoir temperature is shown in Figure 5. These two figures depict how thermionic performance is directly related to collector temperature and cesium pressure.
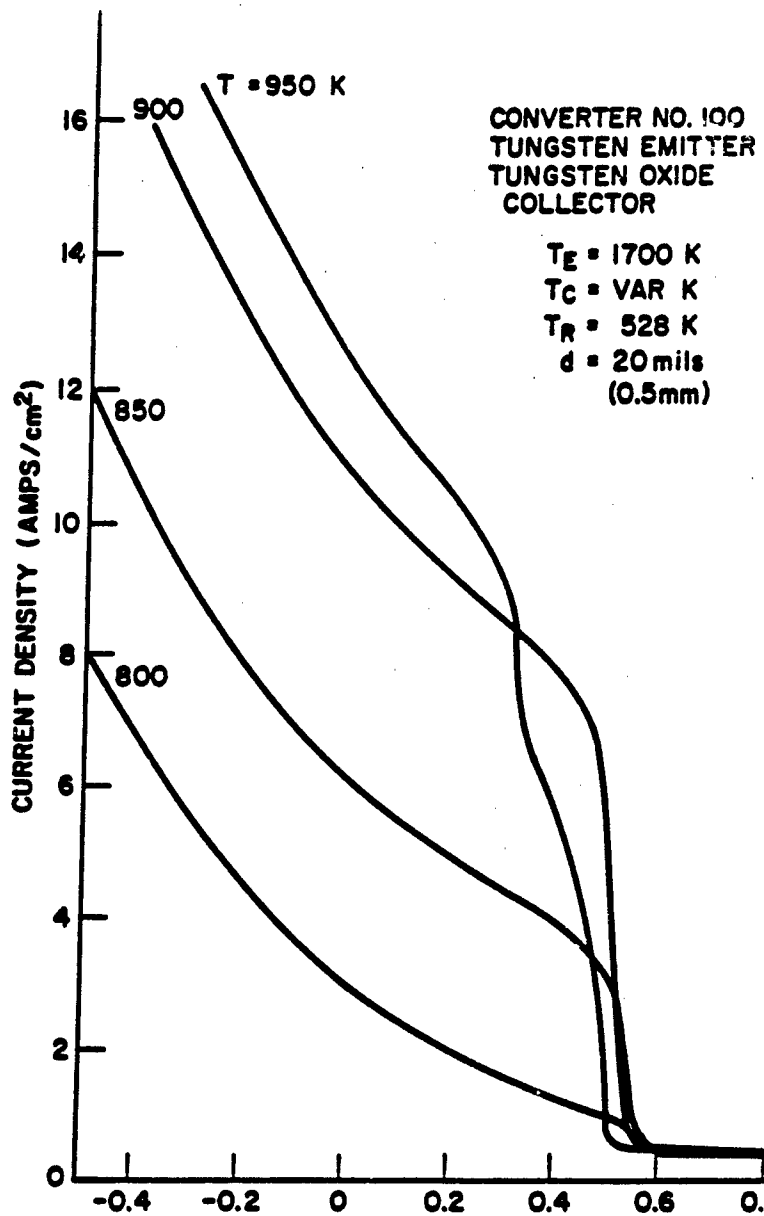
Figure 4.Current-Voltage Characteristics of a Thermionic Diode with Varying
Collector Temperatures(21)

9
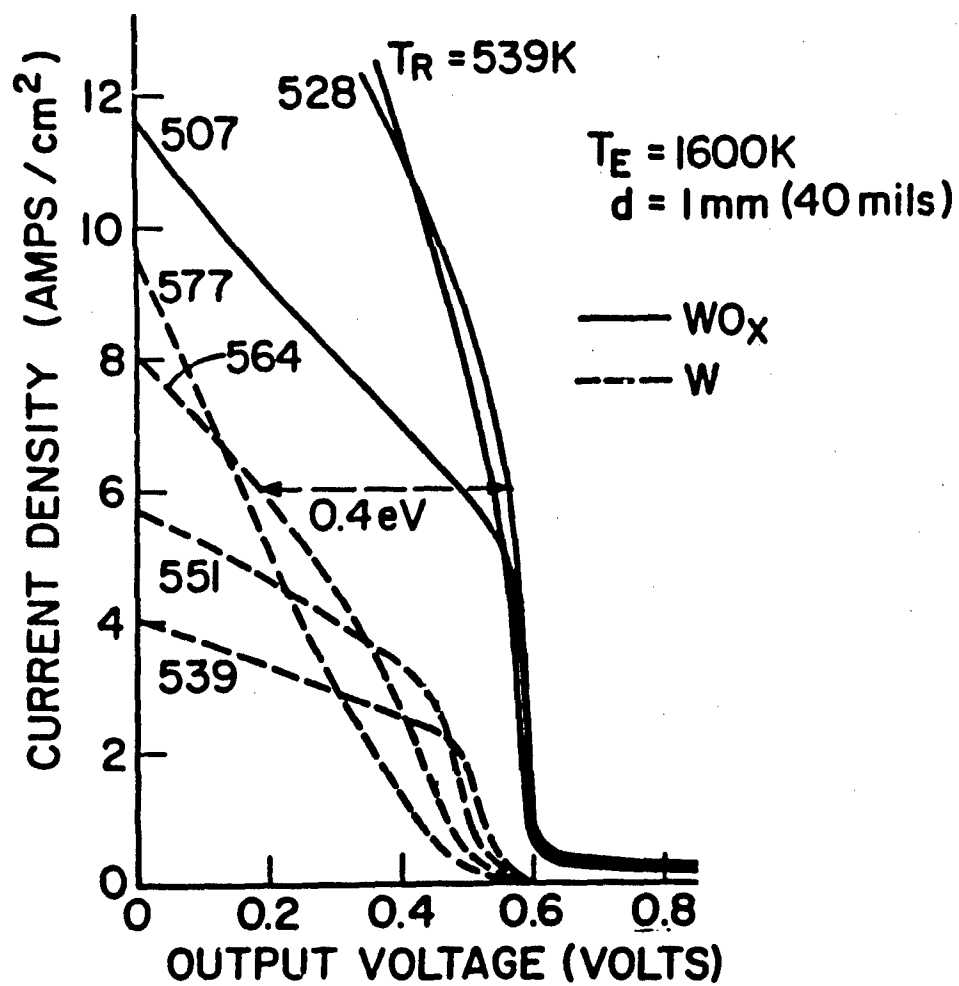
Figure 5. Current-Voltage Characteristics of a Thermionic Diode with Varying

Cesium Reservoir Temperature (11)

10

The optimum power efficiency of the thermionic diode occurs when it is operating just above the knee on the J-V diagram. A thermionic diodes efficiency therefore is directly related to the load voltage it is under. Increasing emitter temperatures also increases diode efficiency by shifting the entire J-V curve up as can be seen by referencing Equation 1. Emitter temperatures are restricted, however, due to emitter material constraints for high temperatures. To optimize thermionic diode efficiency for a given load voltage therefore requires optimization of both the collector temperature and the cesium pressure in order to place the knee of the J-V curve on the required load voltage line as high up the current density axis as possible.

Simple thermionic diodes as discussed here are planar. Various modifications to the diodes shape can be made which allow for compact designs without significantly altering the physics involved, therefore allowing the same equations and relationships to apply. One such variation is the thermionic fuel element.

TFE

Thermionic fuel elements incorporate thermionic converters into actual nuclear fuel elements. A cross sectional view of a TFE is shown in Figure 6. The fuel core usually consists of Uranium dioxide. It is covered by a metal sheath, the emitter. Fission energy in the core produces heat which is conducted outward and heats the surface of the emitter. Encircling the emitter and separated by a small spacing is the collector. This spacing serves as the inter-electrode gap and is usually filled with cesium vapor. The outside of the collector is surrounded by an electric insulator. Coolant channels exist on the outside of this. Coolant, usually liquid metal, flows through the coolant channels to maintain the comparatively low temperature of the collector as compared to the emitter.
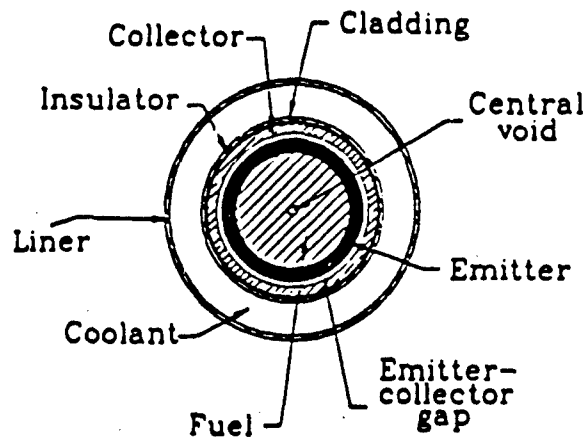
Figure 6. Cross-sectional View of a Thermionic Fuel Element(16)

These TFE's are usually grouped together to form a larger nuclear core. The configuration of the core depends on neutronic considerations more than thermionic considerations. The core often consists of several TFE's surrounded by moderator and reflector material. As each TFE runs axially from the top of the core to the bottom, individual TFE fuel distribution and end cap material tends to determine the axial heat profile of the core whereas the configuration of the core as a whole tends to determine the radial heat profile of the core. Electrically, the TFE's are similar to large batteries, and depending on how they are connected, in parallel or series, determines the current and voltage parameters. Often TFE's are segmented into cells, electrically analogous to a stack of batteries. Such TFE's are called multicelled TFE's whereas one continuous core TFE is called a single cell TFE. A diagram of such a single cell TFE is shown in Figure 7 on the next page.
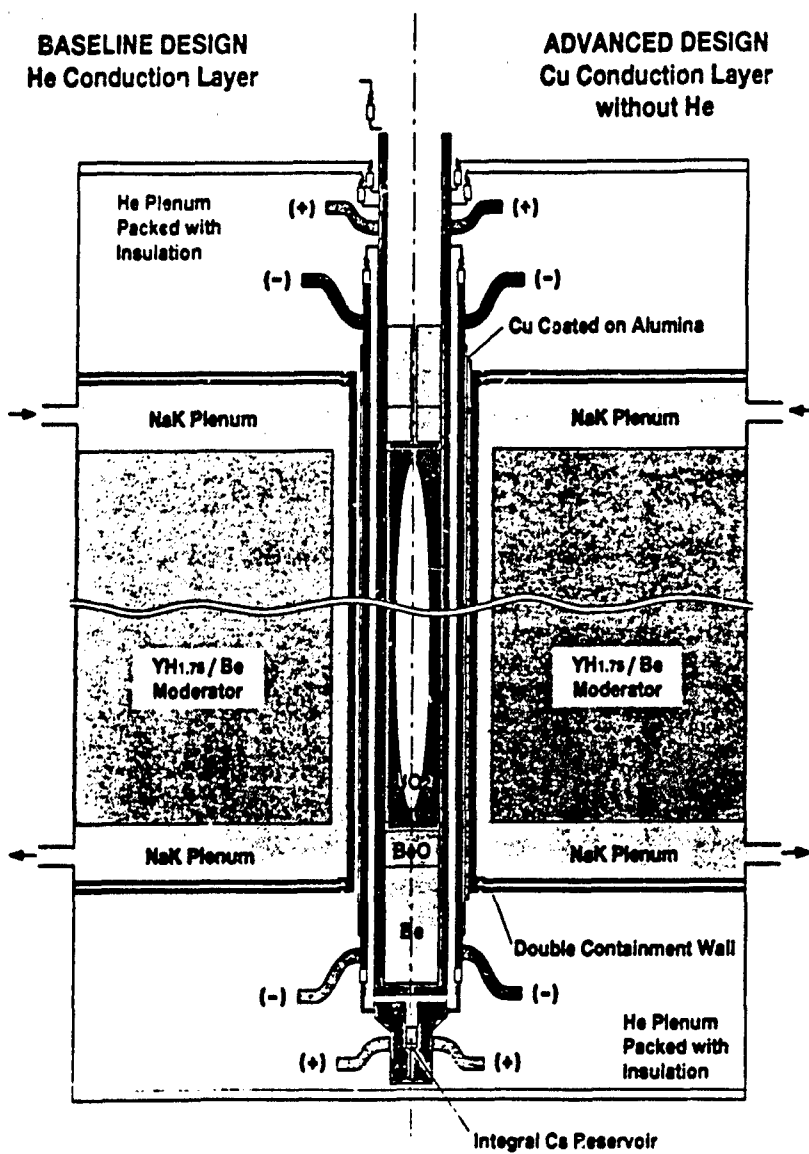
Figure 7. TFE and Core Structure Design for SPACE-R(19)

The ends of the TFE are capped. These caps usually consist of moderator or reflector material depending on neutronic optimization requirements, electrical leads connecting the emitter and collector to the electrical load or another TFE, and a Cesium reservoir and valve system which controls the pressure of the cesium vapor in the gap. The Cesium reservoir pressure is related to its temperature by the second law of thermodynamics. A good empirical approximation, with temperature in kelvin and pressure in torr, is given by: (11:125)

$$p_{Cs} = 2.45 \times 10^8 T_R^{-1/2} \exp\left(-\frac{8910}{T_R}\right) \tag{2}$$

TFE's are usually modeled as long simple planar thermionic diodes. Often they are modeled as a number of smaller simple thermionic diodes connected in series to account for the axial temperature changes which occur in a nuclear core. To model systems of TFE's requires a code which not only takes into account the thermionic efficiency with respect to collector, emitter, and cesium reservoir temperatures, but also a code which accounts for the way that the TFE's are electrically interconnected. TDS is such a code.

15

TDS

TDS was developed to model TFE based nuclear power systems. It operates in a modeling environment called GPS. This environment allows separate models in a system to be combined by treating system parameters as 'flows' of information which go from one model to the next depending on the defined flow path. TDS predicts the electrical currents in thermionic diodes and heat transfer rates across the thermionic diode gaps for large networks of thermionic diodes. Inputs include the materials used with their respective material properties such as emissivity, conductance, and work function; interelectrode spacing; load and lead voltages; cesium pressure in the thermionic gap; and collector and emitter temperatures. It has been designed to model systems with spatially dependent radial and axial temperatures in the thermionic diodes. To do this required combining an existing model, Ignited Mode Planar Thermionic Converter Model (TECMDL), which predicts the performance of a thermionic diode at a point based on component temperatures and current density or gap voltage; and an electrical circuit model, Circuit Solver (CS), which calculates the current density or gap voltage based on the circuitry used. (17:1114)

A combination of these two models is required as both temperature and gap voltage vary spatially along a TFE. Component temperatures vary spatially depending on the power profile of the core. Gap voltages vary axially along the thermionic diode due to the temperature variation and because of resistance losses in the emitter and collector material. TDS solves for a system by interacting the two models through iteration until it converges on a gap voltage solution for the system. Once the two models agree within the designated accuracy, a solution is produced giving the system's temperatures, gap voltages, current densities, and total system electrical performance. (17:1116) A diagram of this process is shown in Figure 6.
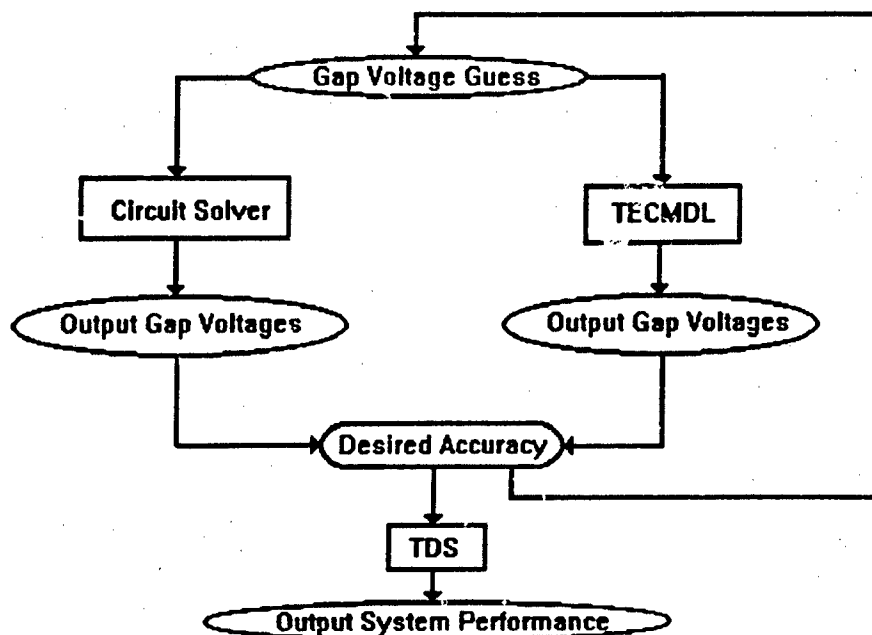
Figure 8. Diagram of TDS Iteration Process

In the CS model the TFE is represented as a simple electrical ladder circuit. The emitter and collector are modeled as a number of resistors in series. The number of resistors represents the number of nodes the user decides to use in modeling the TFE. Each resistor's resistance is a function of the material properties, temperatures, and physical dimensions. The thermionic processes occurring across the gap are modeled as variable electrical power sources as determined by TECMDL. The power sources from TECMDL could either be gap voltages or current densities. The CS model solves for what isn't supplied by TECMDL, either current or gap voltage, by applying Kirchhoff's current law to nodes. CS handles the entire system by creating a matrix made up of conductances and solving for what is required to produce the solution vector provided by TECMDL. The simplified equation is:

$$\bar{\bar{A}}\,\bar{x} = \bar{b} \qquad (3)$$

17

where A is the coefficient matrix made up of conductances, b is the solution vector made up of zeroes (for the current balances) and the values given by TECMDL, and x is the vector being solved for. Figure 9 depicts a sample of how CS would represent a TDS circuit with nine TFE's connected in series and with each TFE being broken into three nodes. A previous study showed that modeling accuracy is directly dependent on the number of nodes used. A one node model underestimated the power output by about 20%.(17:1118-1119) Unfortunately, the more nodes used, the larger the system matrix being solved becomes. The larger the matrix, the longer the code takes to converge on a solution, and the greater the probability that CS and TECMDL will not converge on a solution at all.
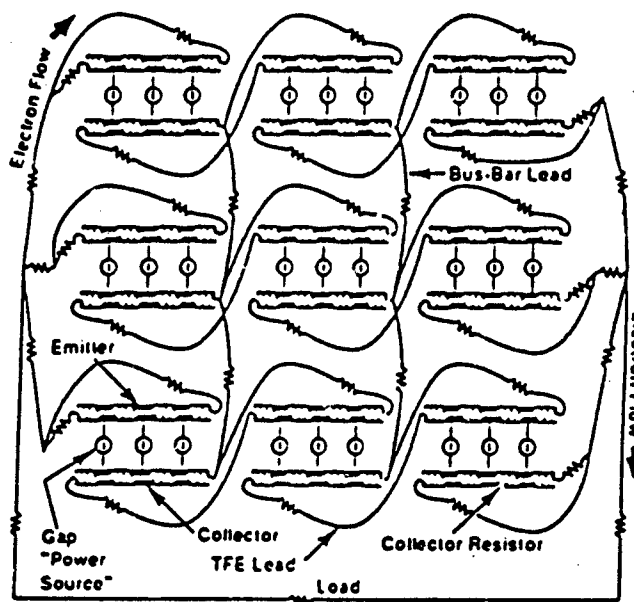
Figure 9. Sample CS Circuit Drawing (17)

TECMDL was developed by John B. McVey at Rasor Associates to do three things:

1. Determine an approximate calculation of converter
   performance and J-V characteristics in the ignited mode.

2. Qualitatively reproduce trends due to changes in
   electrode temperatures, electrode materials, cesium
   pressure, and inter-electrode spacing.

3. Provide insight into the most important physical
   mechanisms which determine converter performance. (23:1)

It takes as inputs the emitter temperature, collector temperature, liquid cesium reservoir temperature, emitter work function, the inter-electrode gap in millimeters, and the current density in amperes per square centimeter. TECMDL returns values for electrode output voltage and the amount that the emitter is cooled due to electron transport and plasma effects.(23:1) This model has been compared to experimental results from several converters and the accuracy is within 10%. This accuracy holds for emitter temperatures ranging from 1600 to 2000 K; collector temperatures ranging from 800 to 1000 K; and a cesium pressure-spacing ranging from 7 to 160 mil-torr or, in terms of a system with an interelectrode spacing of 0.5 mm, a cesium pressure ranging from 0.35 to 8.1 torr.

A diagram of the logic used in the TECMDL algorithm is shown in Figure 10 on the next page. TECMDL begins by reading an input of the electron temperature, T_{eC}, and an electron density, n_C, at the edge of the collector, as well as the corresponding boundary conditions. T_{eC} and n_C initially are guesses that are used as a starting point for the routine. Transport and continuity equations for thermionic converters are then integrated across the plasma to the emitter in one dimension using a standard fourth-order Runge-Kutta algorithm. These equations are developed in Ref. 23 and use the plasma potential, Ψ; the electron current, J_e; the electron heat flux, Q_e; as well as the initial inputted starting point . If the plasma potential at the emitter edge yields boundary conditions requiring a space charge barrier, the electron current at the emitter, J_{eE}, can be determined. If no barrier exists then the Schottky emission current is computed from the electric field at the emitter edge. This process is iterated until heat flux continuity is obtained across the inter-electrode gap; that is that heat flow of the electrons at the emitter, Q_{eE}, equals the heat flow initially defined at the collector edge, $Q_e(0)$. (23:189-190) A diagram of this process is depicted in Figure 10.

TECMDL is used to develop J-V curves for use in system analysis. TECMDL only produces reasonable solutions in the ignited region of a TFE. To get a more complete

20

picture, the routine which uses TECMDL calls on TECMDL to obtain the ignited portion of the J-V curve, and then calls on Unignited Mode Thermionic Converter Model, UNIG, to analyze the unignited regime. UNIG solves for the unignited mode by applying the transport and continuity equations relevant to an unignited mode along with making the assumptions that the electron temperature, ion temperature, and transport coefficients are spatially invariant. Development of UNIG can be found in Ref. 24, Section 3. The results from both UNIG and TECMDL are then splined together to produce one J-V curve.
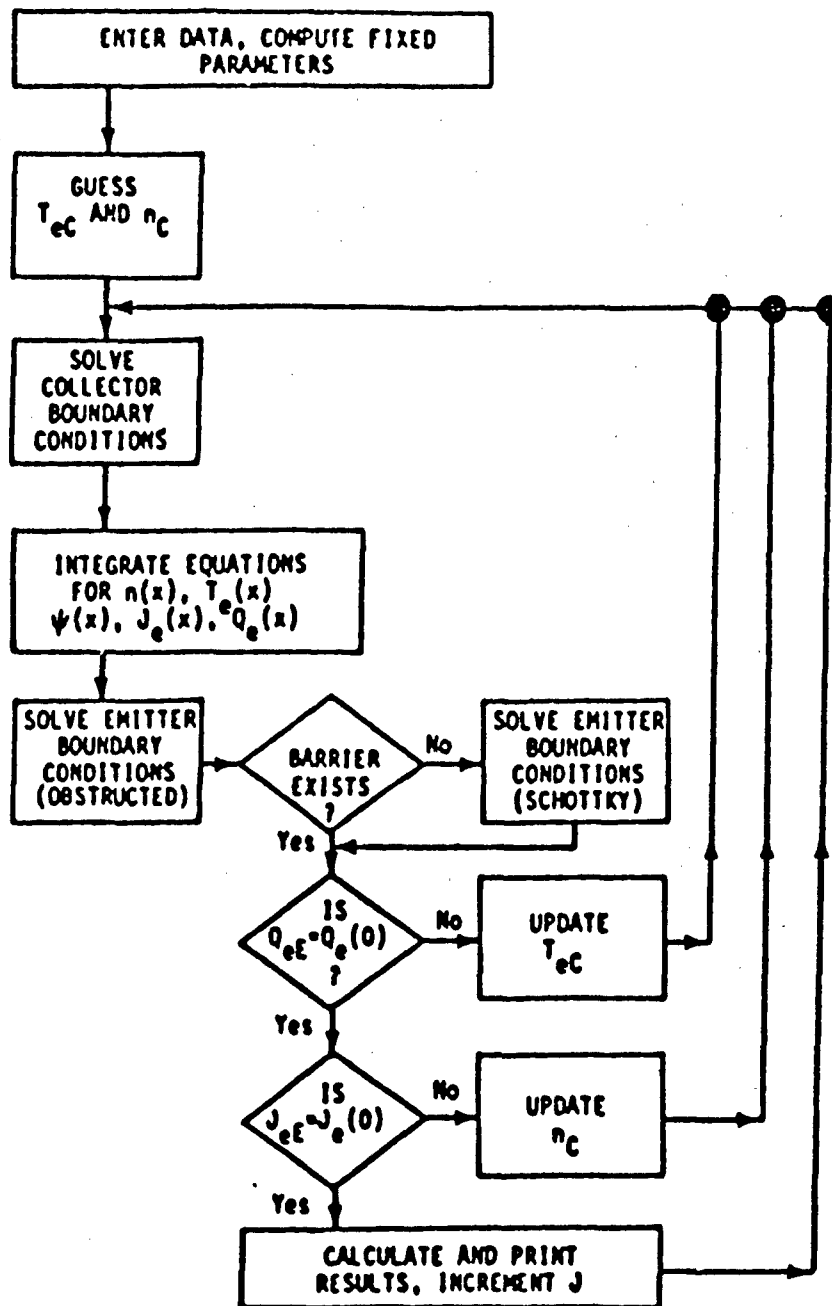
Figure 10. TECMDL Computer Algorithm Logic (20:190)

TOPAZ II

The TOPAZ II power system as of November 1992 is advertised as a 6 kWe space nuclear power system designed and built by the Russians but purchased by the United States for possible use in the Nuclear Electric Propulsion Space Test Mission. It is based on thermionic power conversion utilizing a core of 34 TFE's in series, with an additional three TFE's connected in parallel for the electro-magnetic (EM) coolant pump. The major subsystems of the TOPAZ are the nuclear reactor which contains the TFE's, the radiation shield, the coolant system, the cesium supply system, and the control system. Modeling the performance of the thermionic core required knowledge of the reactor, the coolant system, and the cesium supply system as all three have been shown to have a direct effect on thermionic performance. A table of the major parameters of both the TOPAZ II and SPACE-R systems is shown in Table 1 below.

The nuclear reactor is made up of 37 single-cell TFE's which are fueled by UO_2 fuel pellets 96% enriched in U^{235}. The TFE's are set within axial channels in $ZrH_{1.8}$ moderator blocks, which are canned in a vessel of stainless steel. The core is surrounded by radial and axial beryllium reflectors. The radial reflector also contains three safety and nine control drums which contain a section of boron carbide neutron poison. Neutronics can be controlled by rotating the drums so that the neutron poison is either facing towards the core or away from the core. This allows the TFE emitters temperature to be maintained at between 1773 and 1923 K as long as the coolant system is also operating properly. (6:4-3)

Table 1. TOPAZ II and SPACE-R System Parameters

System Parameter	TOPAZ II	SPACE-R
Electrical Power	6 ± .7 kWe	44 kWe
Thermal Power	115 kWth	611 kWth
Voltage	27 ± 0.8 volts	24 volts
# of TFE's in Core	37: 34 power 3 pump	150
Reactor Coolant	NaK	NaK (primary loop)
Coolant Inlet Temp.	740 K	825 K
Coolant Outlet Temp.	840 K	925 K
Pump Type	Electromag.	Electromag.
TFE Active Length	37.5 cm	35 cm
TFE Emitter Material	Monocrystal MO with 3% Nb	Monocrystal Mo with 7% Nb
TFE Emitter Coating	tungsten W^{184}	tungsten W^{184}
Emitter Inner Dia.	17.3 mm	19.5 mm
Emitter Outer Dia.	19.4 mm	21 mm
Emitter Work Func.	4.95 eV	4.88 eV
Collector Material	Monocrystal Mo	Monocrystal Mo
Collector Inner Dia.	20.6 mm	23.5 mm
Collector Outer Dia.	23.4 mm	25 mm
Collector Work Func.	1.7 eV	
Cs Reservoir Temp.	580 K	566 K
Load Conductance	7.9375 Ω^{-1}	39 Ω^{-1}

The coolant system includes sodium-potassium (NaK) coolant, a single EM pump, stainless steel piping, and a heat rejection radiator. A schematic of it is shown in

Figure 11. The NaK enters the core through a lower plenum at approximately 743 K. It passes through the core were it is heated by the waste heat to approximately 843 K. It exits the core through an upper plenum and then flows through two stainless steel pipes to the radiator inlet collector. The coolant enters the radiator were it separates into 78 small radiator tubes through which the heat is radiated to space. After passing through the radiator the coolant flows into the lower collector where it splits into two paths. One path passes by the Cs unit in order to heat it for nominal operation. The two paths then each branch into three coolant pipes and enter the EM pump from opposite sides. The EM pump pumps the coolant into the lower reactor plenum completing the coolant cycle. (6:4-9)

The EM pump is powered by three TFE's connected in parallel. This allows for failure of one or two of the TFE's without complete system failure. Each TFE failure reduces the power provided to the EM pump by one-third. The EM pump has no moving parts. A diagram of it is shown in Figure 12. The coolant passes through current carrying coils. The current is modulated in a phase staggered fashion so as to produce the pumping action. The operation and efficiency of the pump is determined by the hydraulic resistance, the voltage supplied to the pump, and the temperature of the pump.(6: 4-11)

The cesium supply system (CSS) provides cesium to the TFE inter-electrode gap. It is located between the radiation shield and the upper radiator collector. It is attached to one of the two cold legs of the coolant cycle. This is done to maintain the temperature of the CSS at an operating temperature of ~623 K. The CSS is thermally insulated except for a small radiator located on one end. The cesium evaporates and condenses on the surface of the radiator. Internal to the CSS is a stainless steel "wick" which uses surface tension to transport the cesium and helps maintain constant consumption of the cesium. The cesium vaporizes as it moves down the wick surface. The CSS has a throttle which is

fixeu on the ground to correspond to the cesium optimal pressure as long as the reservoir

temperature is between 623 to 873 K. (6: 4-14)
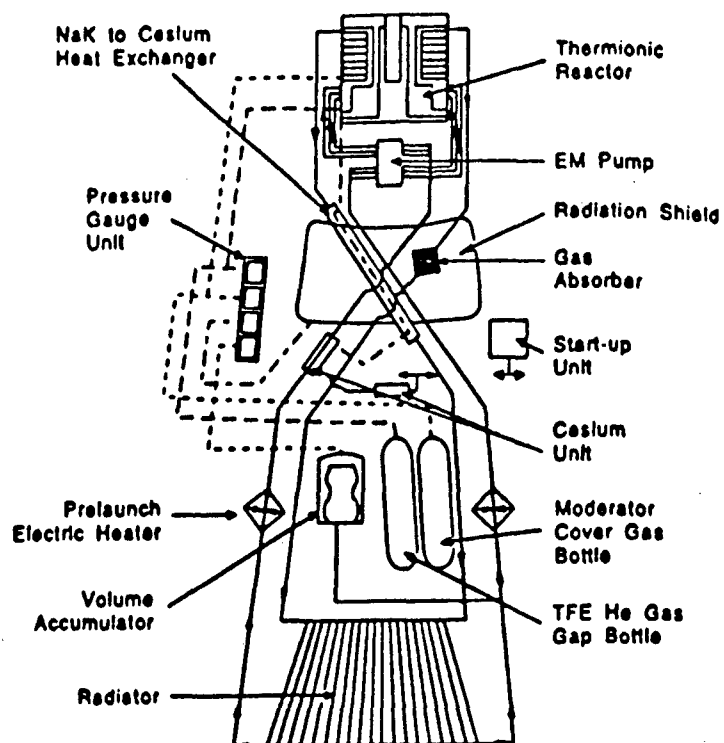
Figure 11. Primary Coolant Loop Flow Schematic (6:4-10)
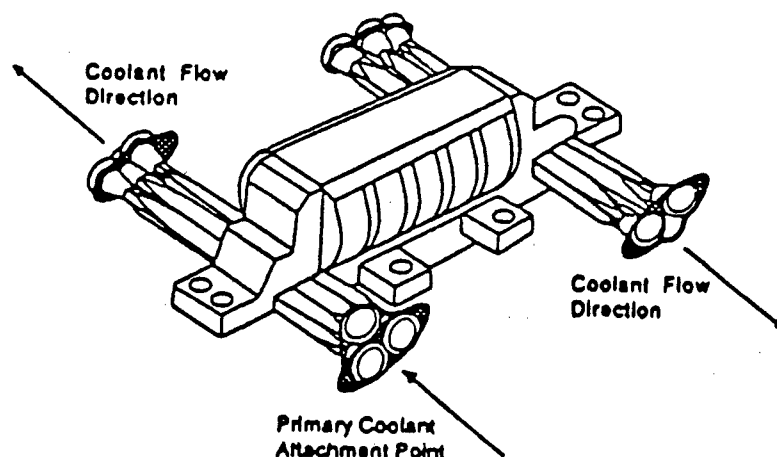
Figure 12. Electromagnetic Pump (6:4-11)

Electrically the TFE's are connected in series as shown in Figure 13. The system is designed to supply 27 volts at a current of 185 amperes to the spacecraft. The ends of the TFE's are electrically isolated and have positive and negative electrical leads. The electrical leads are fabricated from copper and the 34 TFE's are connected in series. Power cables are used to transmit the electric power from the TFE's electrical leads to the electric power distribution system contained in the spacecraft bus. Ballast resistors are installed to dissipate excess electrical power.

35 through 37
TFE Pump Section

1 through 34
TFE Power Supply
System
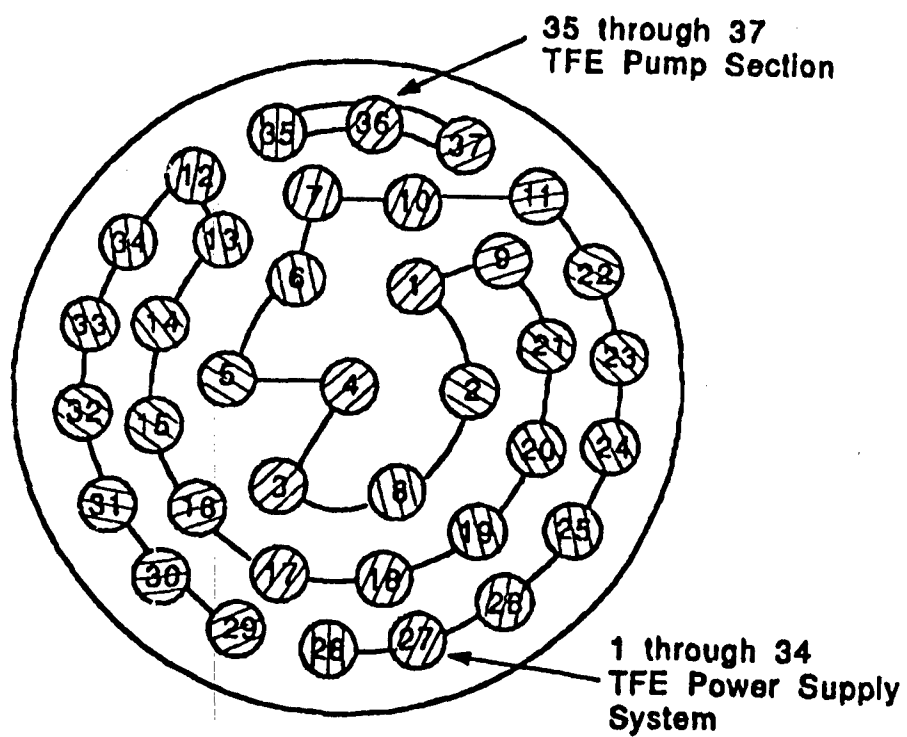
Figure 13. TFE Electrical Connections (6:4-8)

28

SPACE-R

SPACE-R stands for Space Power Advanced Core-length Element Reactor. It is an incore thermionic reactor power system which utilizes 150 single-cell TFE's to produce 40 kWe with a 10 year life time. It's design was based largely on the TOPAZ II core in order to benefit from the large amount of work and studies done on TOPAZ II, and to minimize risk through the use of demonstrated technology.(19:1) The entire system is shown in Figure 14. Similarities between it and TOPAZ II include single cell TFE's with the same emitter and collector materials, a NaK primary coolant loop, an EM coolant pump, and cesium vapor in the gap. Where the two systems differ is in TFE dimensions, fuel distribution in the TFE, in heat pipe radiators, in electrical circuitry, and in overall size. The system parameters are compared to those of TOPAZ II in Table 1.

When modeling the core, the most significant differences between the two systems are the electrical circuitry and core power profile both axially and radially. The other parameter changes can simply be executed by changing the parameter variables' values in the code due to the similarity in TFE design.

Reentry Shield

Launch
Safety Rod

Thermionic
Fuel Element

Control Drum

ZrH$_x$ Shield

LiH Shield

Drum Drive
Motor

NaK Coolant
Loop

Beryllium
Armor

Segmented
EM Pump

Potassium
Heat Pipes

Heat Exchanger

Volume
Compensator

Power
Bus Bar

Carbon-Carbon
Fins
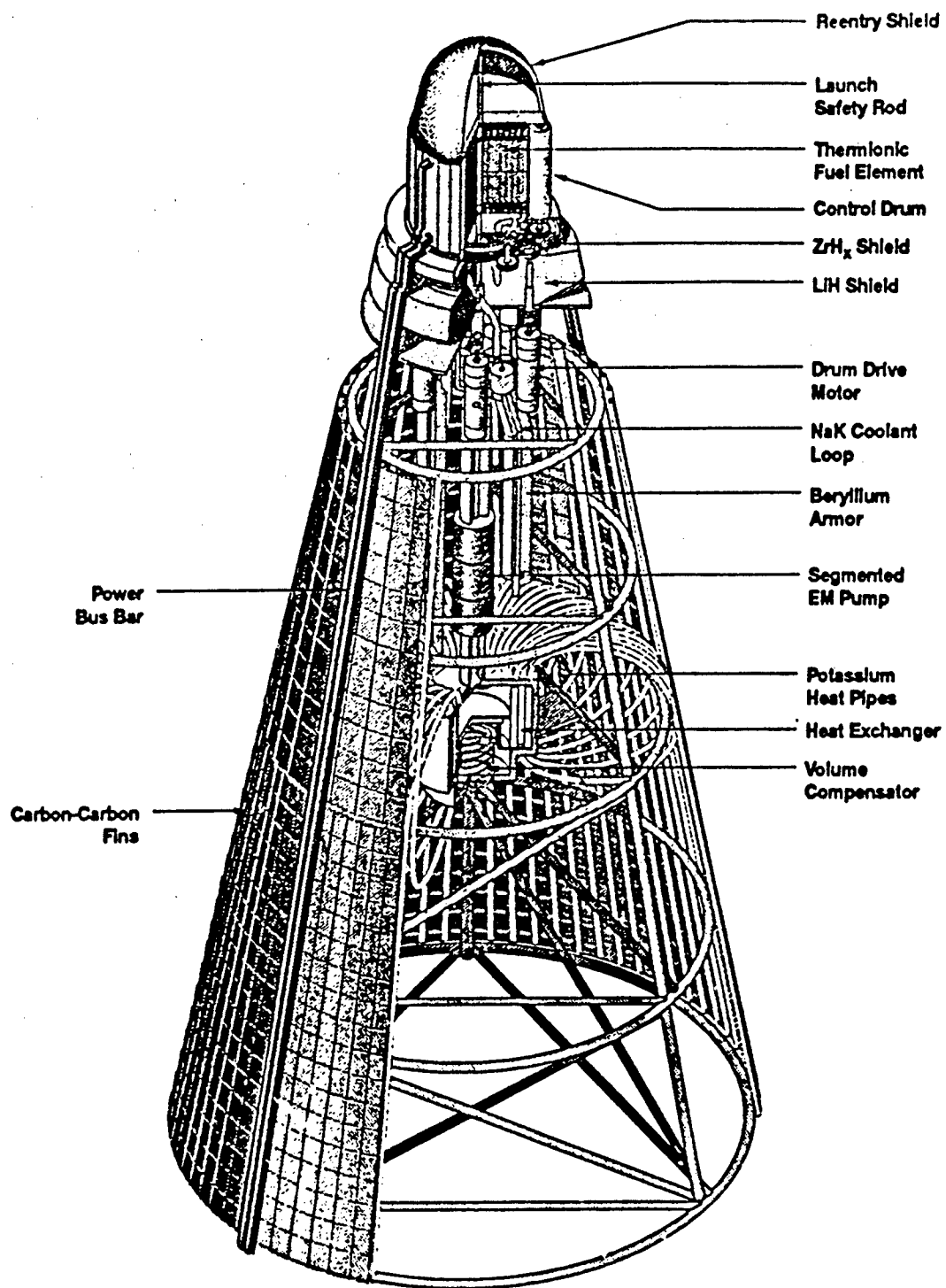
Figure 14. SPACE-R Nuclear Power System(19)

30

Electrical power from the SPACE-R system is taken out from both ends of the TFE's. The TFE interconnections are made in a helium gallery at each end of the core. The TFE's are connected in parallel in groups ranging from 3 to 6 TFE's. The number of TFE's in each group depends on where in the core the TFE's are. In areas of high thermal output smaller groups are used than in areas of low thermal output. 37 of these small groups are connected in series to build up the voltage to 24 volts. A half-core schematic of the TFE interconnection is shown in Figure 15.
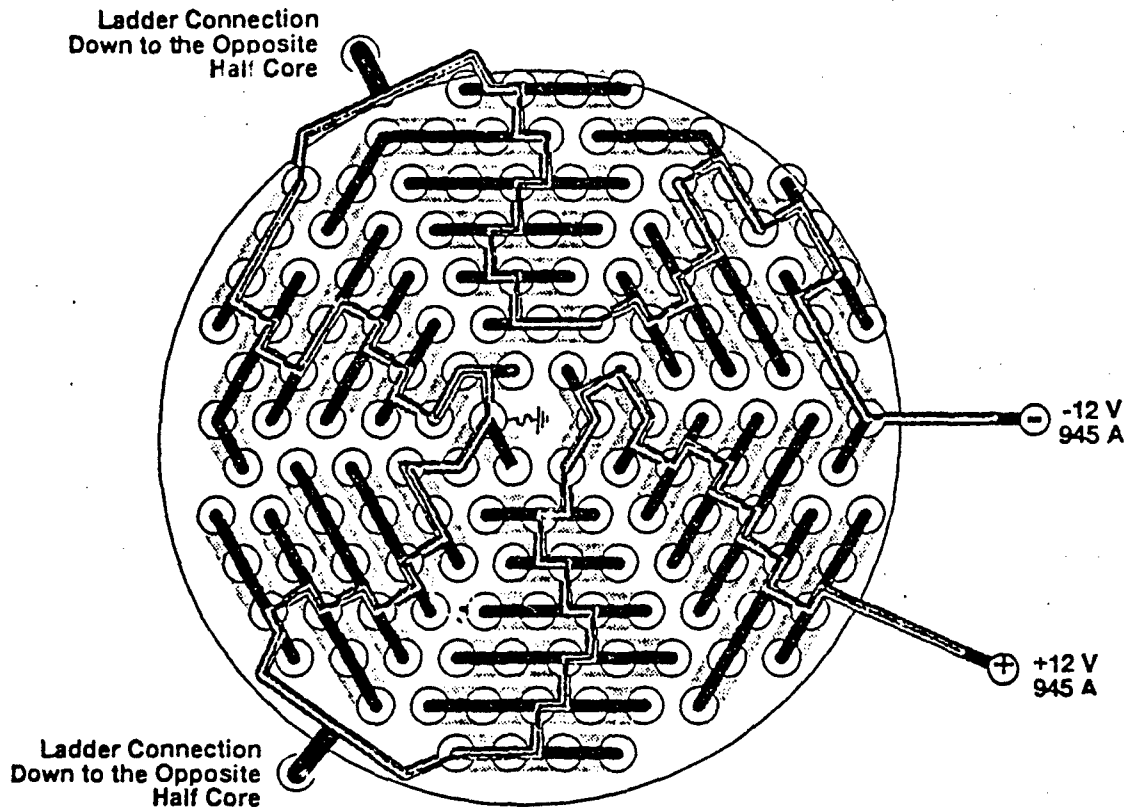
Figure 15. Half Core TFE Interconnection (19:45)

Core thermal power distribution is significantly different than TOPAZ II due to increased use of reflectors at the radial perimeter of the core and the use of a varying fuel density in the TFE. The increased use of reflectors at the core perimeter creates an increase of thermal activity at the perimeter which is not present in the TOPAZ II. The radial profile is shown in Figure 16. Additionally, by varying the fuel smear density axially with the greatest density at the ends and decreased density at the center of the TFE, as shown if Figure 17, the axial power profile is almost completely flat as is shown in Figure 18.
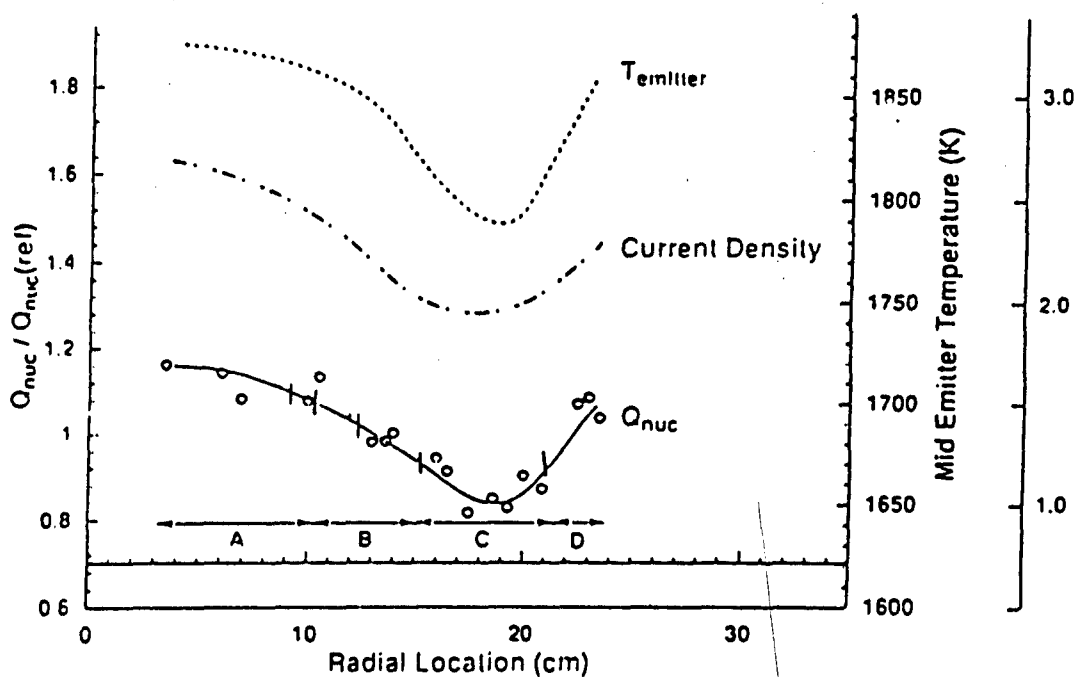
Figure 16. SPACE-R Radial Power Profile (19:48)
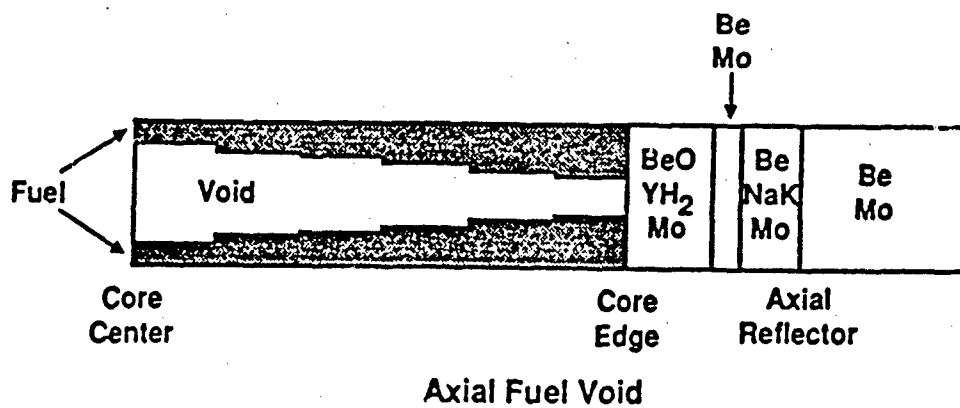
Figure 17. Illustration of Axial Fuel Void in TFE (19:118)
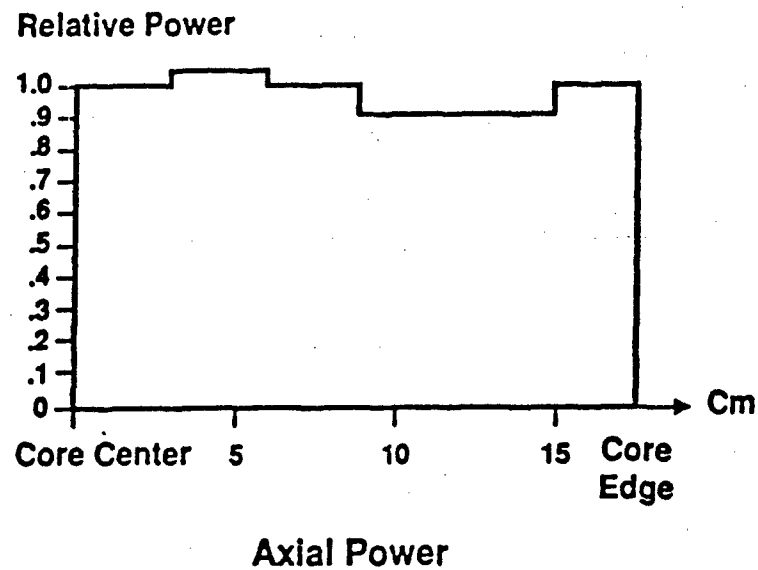
Figure 18. SPACE-R Axial Power Distribution (19:118)

33

The EM pump is similar to that described in the TOPAZ II. It is composed of three sections allowing for system redundancy. Each section can provide up to 50% of the pumping required, thus allowing the system to operate normally with one section failed. Two section failure would decrease coolant flow by 50% and the result would be an increase in coolant temperature thus causing increased degradation rate of the coolant loop.(19:52)

Design of the integral cesium reservoir has not yet been specified. Many suggestions exist from using a system similar to that in TOPAZ II to using a graphite Cs reservoir or a metal matrix cesium reservoir. The advantage of the new designs being worked on is a more stable Cs pressure which is less dependent on reservoir temperature.

III. Parameter Studies

Introduction

Four parameter studies were conducted on the TOPAZ II nuclear power system. These studies determined system performance and efficiency while varying the following:

1. The coolant flow inlet temperatures.

2. The rate of coolant temperature change.

3. The power profile of the core.

4. The cesium reservoir temperature.

An input file describing the TOPAZ II system was built based on published system parameters. A thermal profile of the core was obtained from a MCNP study conducted at Phillips Laboratory(1) and converted into an array for input into the model. Parameter study ranges and configurations were determined by the test desired and the ability of TDS to converge on solution. Additionally, initial guesses of emitter temperature and gap current density were varied to help the code converge on a solution for the TOPAZ II. Individual solutions were then checked for reasonableness and then compiled for analysis of the parameter studies.

TOPAZ II System Modeling in TDS

TDS allows for system variable inputs to be made in several different ways. Variables can be defined in the original TDS FORTRAN code before it is compiled for use in the GPS environment. Additionally, variables can be defined in the GPS interface code which interfaces TDS to the GPS code. The final method is to define the variables in the problem statement which calls on TDS. This final method is the easiest method of defining variables likely to be changed for parameter studies.

With the exception of the temperature, voltage, and power profiles; the TOPAZ II system parameters outlined in Table 1 were defined in the GPS interface code. Emitter temperatures, collector temperatures, and TFE power profiles are arrays. Their size is

determined by the number of nodes per TFE being used as each node has a corresponding set of parameters. Therefore, their values were introduced in the problem statement. Additionally, variables which were changed during the parameter studies were also defined again in the problem statement. Variable definitions in the problem statement take precedence over variables defined elsewhere.

The problem statement was based largely on a problem statement provided by Ralph Peters at Phillips Lab.(18) It is called 'q_8_p'. It originally was used to conduct a parameter study that determined the electrical system power for different peak thermal powers. 'q_8_p' allows both the collector temperature profile and the core thermal power profile to be defined for either an eight or three node problem. The initial guess for the emitter temperature and gap current arrays are also built. 'q_8_p' then utilizes a sophisticated version of the "fixed point iteration" method to help GPS converge on the system solution. In essence, it breaks the system problem into smaller problems which GPS can solve by slowly increasing the desired accuracy as GPS accuracy improves. It also varies the GPS iterative step size depending on how quickly GPS converges on an intermediate solution.

The TDS problem statement provided by Phillip's Laboratory, 'q_8_p', was updated for the parameter studies conducted here. The thermal power profile was redone based on recent MCNP studies conducted at Phillips Lab (1). It analyzed the TOPAZ II core as it is found at the beginning of life (BOL). The MCNP results yielded axial thermal power profiles for TFE's in each of the four radial regions discussed earlier and depicted in Figure 19. The MCNP study divided each TFE into 20 regions. These solutions were converted into 3 and 8 region results for use in the 3 and 8 node studies conducted.

Coolant Flow Inlet Temperature Study

The coolant flow inlet temperature study was conducted to see how coolant temperatures affect thermionic performance. Coolant temperature rise is something which would occur with some kind of coolant cycle problem such as radiator damage or degradation. If this were to occur, the coolant temperature at the inlet of the nuclear core would rise above the design temperature, causing a rise in the collector temperatures of approximately equal magnitude due to high heat transfer coefficients in the collector and coolant.

As coolant flow has not yet been included in the TDS model, the coolant temperature is represented by the collector temperature. The collector temperature at any given point is closely related to and slightly higher than the coolant temperature at that same point. As the coolant passes through the hot core it increases in temperature as does the collector temperature. Phillips Laboratory provided a normal beginning of life coolant temperature axial profile with the 'q_8_p' code (18). The average collector temperature rise per node of the 8 node profile was given to be 12.5 K. The increase in the coolant temperature of the inlet flow was modeled by raising the temperature of each TFE's first node while maintaining the same temperature increase between each of the remaining seven nodes.

For the parameter study, the initial collector temperature was increased by increments of 50 K until the TDS code reached a point were it could no longer converge on a solution. This point was reached when either the parameters exceeded TECMDL's range or when the high collector temperatures drove the TFE's to a primarily unignited mode where code stability between TECMDL and CS is poor. The problem was modeled in the updated 'q_8_p' routine using 8 nodes per TFE. As the input collector temperature array was being varied, the 8 node profile was used instead of the three node profile in

37

order to better track temperature changes across the TFE. The only variable changed for this parameter study was the collector temperature profile.

Rate of Coolant Flow Study

The purpose of this study was to model how coolant pump degradation would affect system performance. As earlier stated, the coolant pump is an EM pump powered by three TFE's connected in parallel. The failure of any of the pump's TFEs would result in a decrease in pump power by 1/3. This would cause a decrease in coolant flow rate. As the coolant flow rate decreases, its time in the nuclear core increases. This results in a greater increase in coolant temperature per node. As coolant temperature and collector temperature are directly related, the result is a greater increase in collector temperature per node.

To model pump degradation, the input array of the collector temperatures is changed by increasing the collector temperature increase between nodes in each TFE. This causes a greater increase in collector temperatures from one end of the TFE to the other while maintaining the same inlet temperature. The first node collector temperature is kept constant as the extended time in the hot core is compensated for by the extended time in the heat radiator. Also, space radiators are more efficient at higher temperatures. All other model input parameters are left unchanged. Temperature increases between nodes of 12.5, 20, 25, and 40 K were modeled. These temperature increases were arbitrary and were based on the ability of TDS to solve the model. They were chosen to cover as wide a temperature range as possible.

Core Power Profile Study

The core profile of the TOPAZ II modeled was based on MCNP results. These results were based on known core dimensions and material characteristics. Simple

changes such as adding or repositioning neutron reflectors or poisons could significantly alter the neutron flux spatial profile and thus the thermal profile of the core. Another variable which can change the thermal profile would be how the fuel is spread in the TFE core. As thermionic performance is directly related to emitter temperatures, small changes in a thermal profile could have an effect on thermionic efficiency of a system.

The thermal profile provided by Phillips Laboratory is shown in Figure 19 as the 'Normal' profile. This illustrates how the thermal power at the TFE's axial center is nearly twice that found at the ends of the TFE. As thermionic efficiency tends to increase with increased emitter temperature, the TFE ends on the normal profile will produce less electric current then the TFE center were it is the hottest. Additionally, if the TFE emitter ends are at too low a temperature they could be in the unignited region and be very inefficient. Flattening a profile could raise the ends of the TFE's thermal profile high enough to raise unignited regions to ignited regions.

In this parameter study, the normal power profile was flattened in a variety of ways as outlined in Figure 19. The profiles were chosen to cover a range of profiles from the normal peaked profile results of the MCNP study on TOPAZ II(1) to a completely flat axial profile which was modeled and predicted for the SPACE-R system(19:118). Actual modeling of how the core would be modified to achieve the different profiles was not done, but the profiles are assumed to be reasonable due to actual modeling of the profiles on each end of the profile spectrum. All of the power profiles have the same total thermal power in order to compare profile efficiencies. In reality, adding reflector materials to flatten the thermal profile would also increase the systems total thermal power. If total system mass is conserved, the extra reflector mass would require fuel mass to be removed, decreasing the total thermal power. As space nuclear cores are designed to optimize thermal power with respect to mass, the assumption of using the same total thermal power is therefore conservative.

Profiles for Region 0
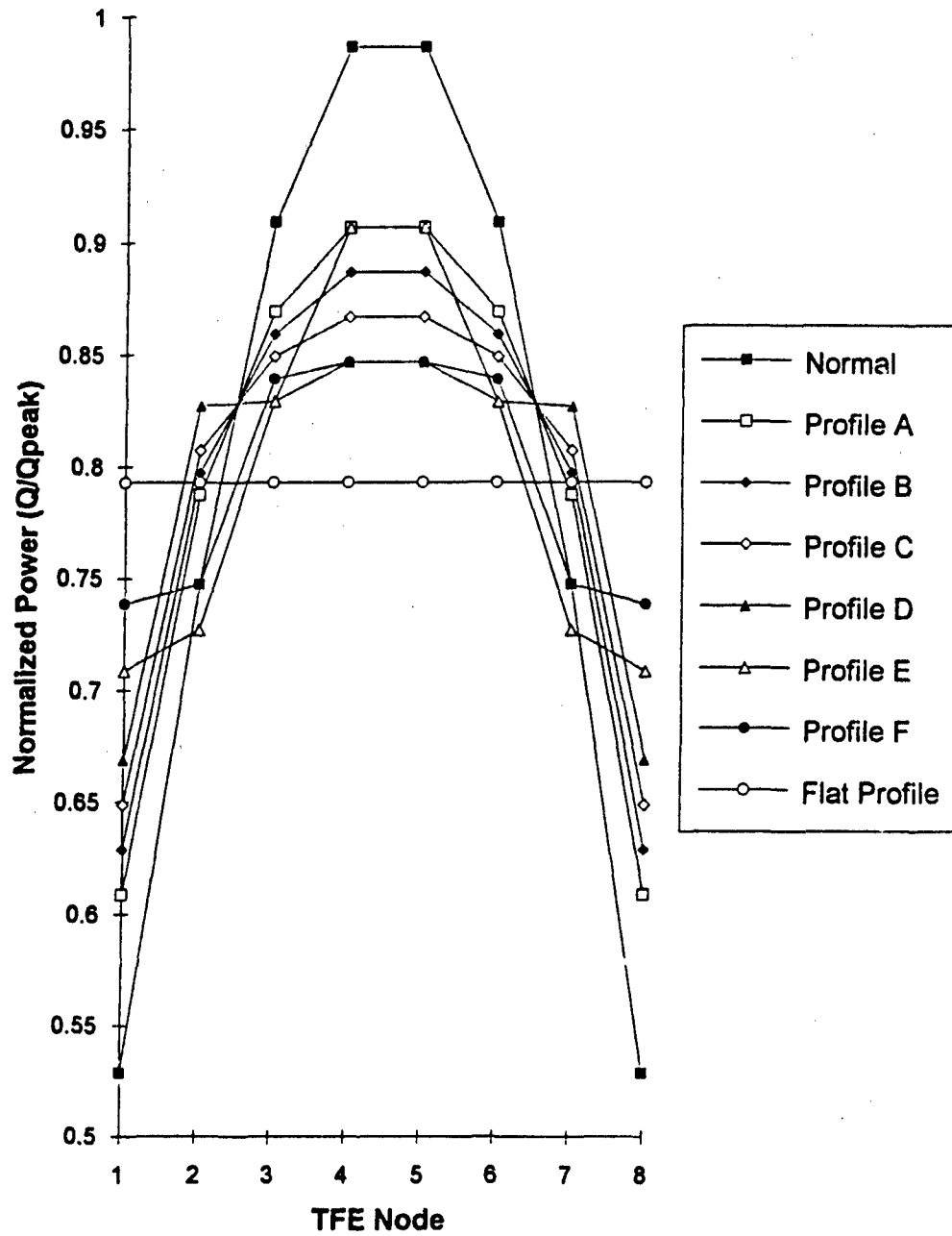
Figure 19. Axial Thermal Profiles for 8 Node TFEs

Cesium Reservoir Temperature Study

As discussed earlier, cesium reservoir temperature has a direct effect on cesium pressure, and cesium pressure directly affects thermionic performance. The TOPAZ II cesium reservoir has a throttle which controls the cesium gap pressure as long as the reservoir temperature is between 620 K and 870 K. At these temperatures published results claim it will maintain a cesium gap pressure of at least 2.0 torr. This pressure corresponds to a reservoir temperature of 580 K. If this throttle should fail then the cesium pressure would be higher than the selected optimum pressure. If the reservoir temperature does not reach 620 K, possibly due to a problem with the coolant loop which heats the reservoir, the optimum cesium pressure might not be achievable.

The cesium reservoir temperature was changed while holding all other parameters constant. The 3 node TFE model was used as it is more likely to converge on a solution than the 8 node model used for the other three studies. This is due to the matrix built in the CS model. As it increases in size, the probability of it solving the problem decreases. The increased accuracy of the 8 node model was not necessary as the input temperature profile and the thermal profile were not being changed in this parameter study. The parameter for the cesium reservoir temperature is converted to the cesium gap pressure by applying Equation 2, which assumes that the cesium vapor pressure is a direct reflection of the reservoir temperature. This corresponds to a system were the cesium pressure throttle is broken and open. Reservoir temperatures in this study ranged from 565 K to 623 K as this was the range that TECMDL was limited to.

41

IV. Results and Analysis

Each parameter study could be broken into multiple system model runs. The results of each successful run, i.e. a run where the modified 'q_8_p' model was able to converge on a solution, appeared in a format like that shown in Appendix C. Relevant data from the individual runs were then grouped together for the parameter study. A spreadsheet was then used to compile the data and present it in graphical form. Results from the four parameter studies are discussed below as well as a discussion on the validity of the modified 'q_8_p' TOPAZ II system model.

TOPAZ II System Model Results

The modified 'q_8_p' results were compared with published Russian results for the TOPAZ II system (6:4-2). Table 2 is a table with 'q_8_p' results and published TOPAZ II results. The results of the 'q_8_p#1' model as compared to published results shows the electrical power performance results that were from 'q_8_p#1' are 30% to 45% low depending on where in the published electrical power range you are looking. The total thermal power calculated in 'q_8_p#1' indicates that the initial power profile based on MCNP results is 12% lower than that advertised for TOPAZ II. As the power profile input is normalized based on the region where power flow of the entire system peaks, simply raising the value of the thermal power for the peak region allows the entire thermal power profile to be raised. The Q_{peak} value was raised from the MCNP calculated value of 17.32 W/cm^2 to 19.7 W/cm^2. This raised the model, now called 'q_8_p#2', total thermal power results to those published for BOL. The new model now underestimates the electrical performance by only 10%.

Table 2. Modeled Results vs. Published TOPAZ II Results

Parameter	Published	q 8 p#1	q 8 p#2
Thermal Power	115 kWth	101 kWth	115 kWth
Electrical Power	6 ± 0.7 kWe	3.74 kWe	4.73 kWe
Load Voltage	27 ±0.8 volts	21.7 V	27.9 V
Q peak	--------	17.32	27.0
T(Emitter) Range	(1773 to 1923 K)	(1618 to 1796 K)	(1725 to 1950 K)

Several factors account for the disagreement between modeled values and published values. The model breaks each long TFE into smaller thermionic diodes. This segmentation neglects the fact that the cesium plasma in the interelectrode gap is more or less continuos from one end of the TFE to the other. The effect of this is that the characteristics of the plasma are homogenized to a degree. This means that a node TDS models as operating in the unignited mode may actually be operating in the more efficient ignited mode due to plasma characteristics carrying over from a hotter region. The net effect of dividing the TFE for a peaked thermal profile is an underestimation of the system efficiency. Additionally, the TECMDL code used in TDS tends to underestimate thermionic performance for emitters at higher emitter temperatures like those that TOPAZ II operates at.

As new information is now being released by the Former Soviet Union on the performance of TOPAZ II, both 'q_8_p#1' and 'q_8_p#2' models were used in conducting the parameter studies. Using both models also allows for a comparison of how total thermal power affects system performance.

Coolant Inlet Temperature Study Results

The coolant inlet temperature study tested what would happen to the system if coolant temperatures flowing into the reactor core increased above those published. Results of this study using 'q_8_p#1' are shown in Figure 20.

Figure 20 illustrates that initially, as the collector temperature rises, system efficiency also rises by up to 6%. This is due to the fact that the emitter temperature also rises as collector temperatures rise. The relatively smaller rise in emitter temperature has a greater positive effect than the negative effect that the larger rise in collector temperature has.
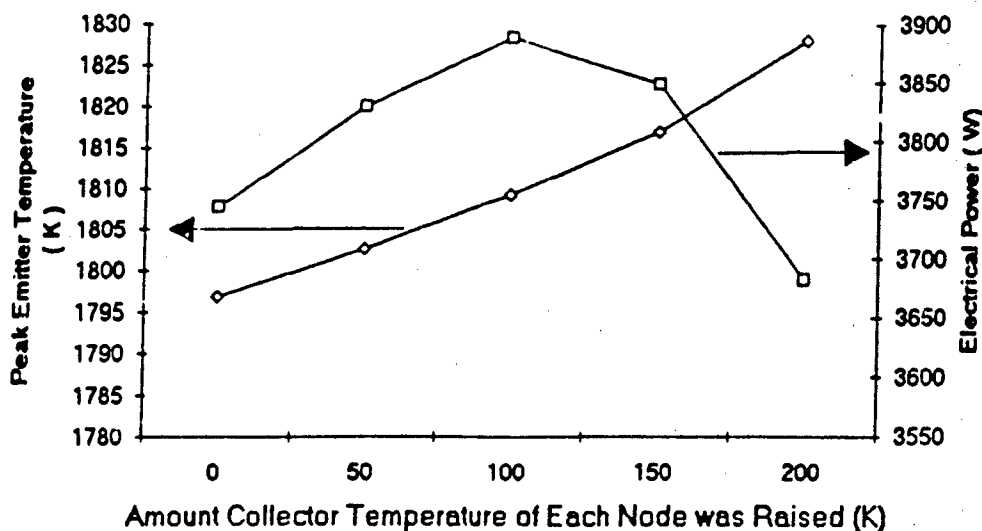
Figure 20. Plot of the Amount the Collector Temperature was Raised vs. Emitter
Temperature and Electric Power

After the inlet temperature is increased approximately 100 K, the system efficiency
peaks and further collector temperature increases result in decreased system efficiency.
This indicates that increasing the emitter temperature is having less positive effect than the
detrimental effect of increasing the collector temperature. The negative effect of raising
collector temperatures can be seen by looking at how J-V curves change with changing
collector temperature. Figure 4 depicts such a study. To optimize a system, the load
voltage is set so the thermionic diode operates at the knee of the J-V curve. As the
collector temperature is raised, the knee of the J-V curve begins to shift further left and
further up. As the output load voltage is not changed, the thermionic diode operating
point soon drops well below the knee and the thermionic diode will begin to operate in the
inefficient unignited mode. This effect was verified by going into TECMDL generated

45

J-V plots such as that used in TDS and comparing them to results from a given TDS solution set. This could be done as the output from 'q_8_p' include voltage, temperature, and current density information for each node of every TFE.

A similar study was done using 'q_8_p#2'. It had difficulty determining a solution when collector temperature arrays were increased by more than 100 K. For temperature increases up to 100 K, the results were similar for both versions of the model with 'q_8_p#2' yielding higher efficiencies. Figure 21 compares the results of the two models. As TDS typically encounters difficulties when thermionic diodes drop below the knee of J-V curves, a decrease similar to that in 'q_8_p#1' is expected beyond 100 K for 'q_8_p#2' as well.
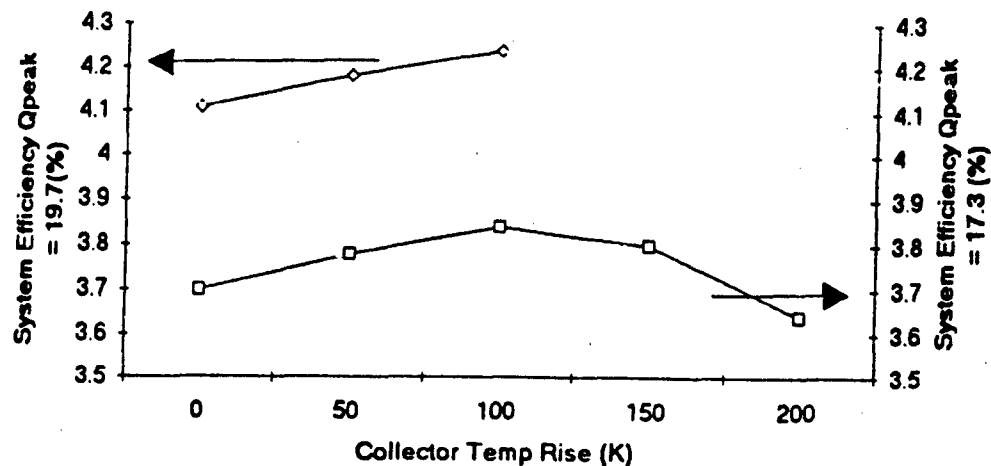
Figure 21. System Efficiency vs. Amount Collector Temperatures are Raised for

Models #1 & #2

Coolant Flow Rate Study Results

The purpose of the coolant flow rate study was to model what the effects of slowing coolant flow would be on the TOPAZ II system. This was done by increasing the amount the collector temperature rises from the bottom node to the top node. Results of the study are summarized in Figures 22 and 23, with dT representing the temperature change the collector undergoes between nodes. Figure 22 shows how emitter temperature increased with collector temperature increase. The increase in emitter temperature is relatively small with respect to collector temperature increase.

Therefore the analysis made in the first parameter study should apply here also. This is verified in Figure 23 which depicts how the system efficiency peaks with increased ΔT per node at approximately $\Delta T=25$.
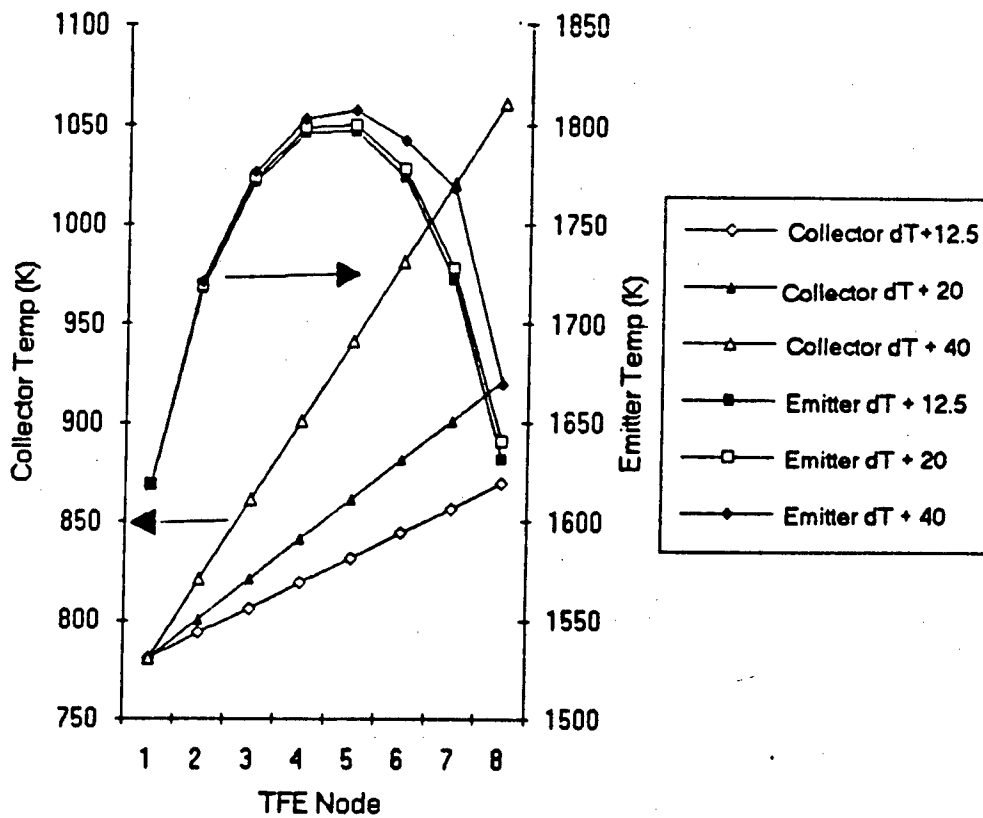
Figure 22. Collector and Emitter Temperature Rise Across the TFE
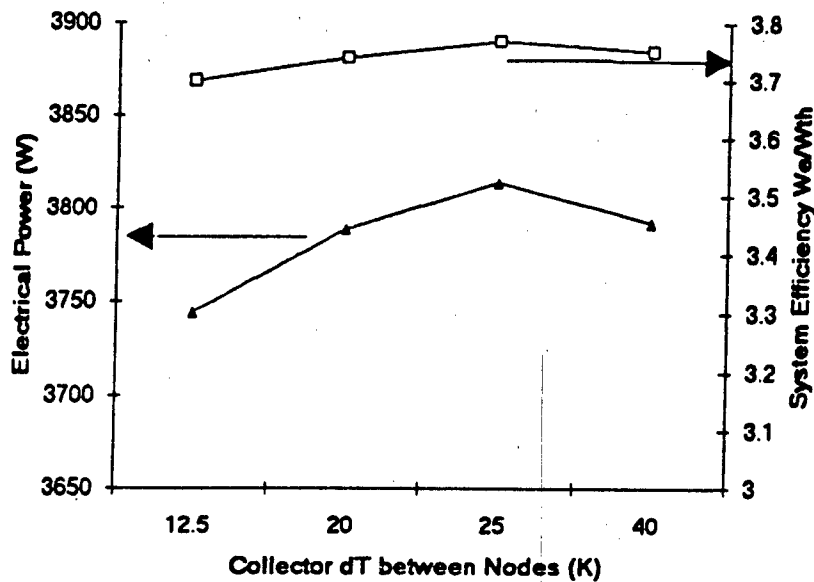
Figure 23. Graph of System Efficiency and Electrical Power vs. Collector ΔT per Node

The reasons for this peaked system efficiency profile are the same as those discussed in the last parameter study. Emitter temperature increase due to increasing collector ΔT initially has a greater positive effect than the negative effect that the increased collector temperature has. As collector ΔT rises, the diodes respective J-V curve begins to shift left. Eventually the J-V curve has shifted far enough left so that the diode is operating in a very inefficient and possibly unignited mode.

Power Profile Study Results

The purpose of the power profile study was to determine the effects that flattening the thermal power profile would have on system efficiency. Figure 19, previously discussed, depicts the various profiles studied. Figures 24 and 25 depict the amount of electrical power produced per profile as well as the peak emitter temperature produced by that profile. Figure 24 is based off the 'q_8_p#1' model and Figure 25 is based off the 'q_8_p#2' model.
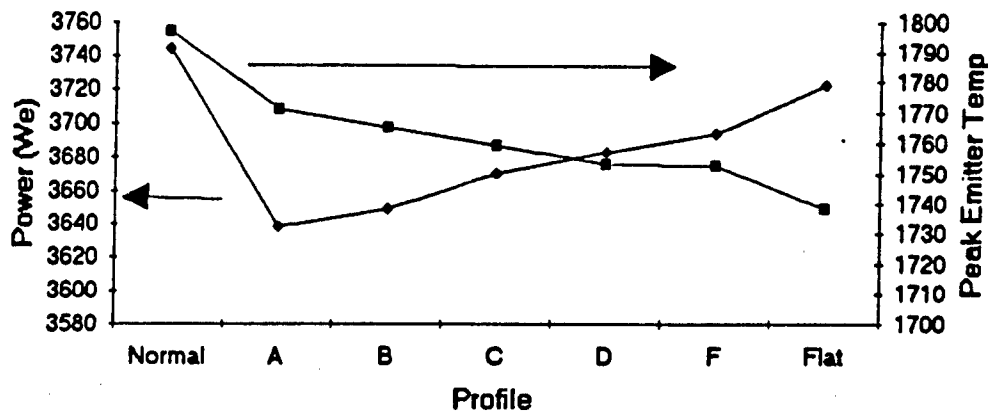
Figure 24. System Electric Power and Emitter Temperatures for Different Profiles

(q_8_p#1)
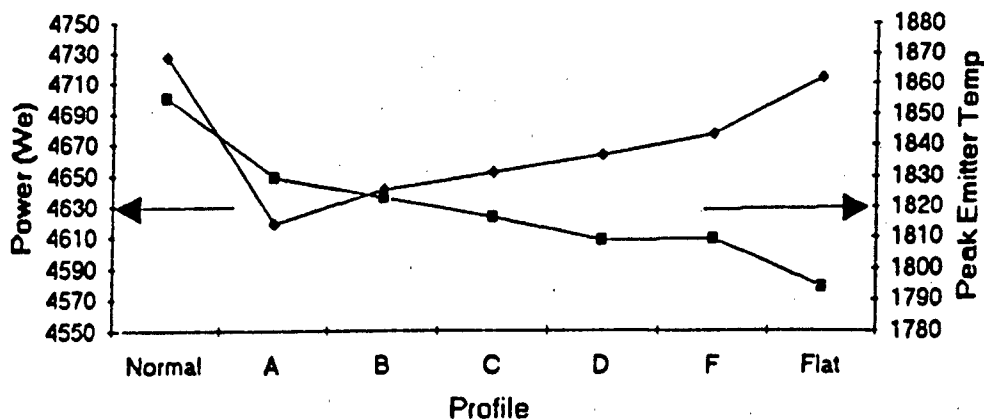
Figure 25. System Electric Power and Emitter Temperatures for Different Axial
Power Profiles (q_8_p#2)

Figure 24 and Figure 25 illustrate how flattening the power profile usually increases

the total electric power produced and decreases the emitter peak temperature. This is due

to the fact that the TFE emitter temperatures at the ends of the TFE are raised to the point

that they are now operating in the ignited mode instead of the unignited mode. When the

increase in thermionic performance of the TFE ends is greater than the decrease in

thermionic performance of the TFE center, a net increase in system performance occurs.

The most efficient profile is the normal profile which is also the most peaked. This is due

to the fact that the center four regions of the normal profile are operating above the knee

on their respective J-V curves. Additionally, their respective J-V curves are shifted up due

to increased emitter temperatures in the core, also allowing them to produce more power.

This compensates for the lack of efficient thermionic conversion on the ends where the

TFE's are operating at a lower efficiency. Even at the ends of the most peaked profiles, the thermionic diodes were operating in the ignited mode, although well below the optimum operating point. Their efficiency was affected more by the lower emitter temperatures shifting their respective J-V curves down than by their actual location on the J-V curves.

As none of the profiles modeled were operating in the unignited mode, their system efficiencies were very similar. The difference between the most efficient and least efficient profiles was less than 2.5%. The difference between the perfectly flat profile and the profile used in TOPAZ II is less than 0.3%. These are differences that would be difficult if not impossible to measure in a real system. Furthermore, as previously mentioned, the TDS code underestimates actual performance as it does not account for the homogenizing effect that the cesium plasma has in the inter-electrode gap. This effect would be more apparent in a peaked profile and would be virtually nonexistent in a flat thermal profile where emitter temperatures, current densities, and gap voltages are nearly equal. It is possible that the difference in the efficiency of the normal peaked profile that TOPAZ II uses and that of a completely flat axial profile might be even greater than the model showed. This suggests that the efforts being made to flatten the power profile axially in systems such as SPACE-R are not required as the system runs more efficiently with a peaked profile.

Results of Cesium Pressure Study

The cesium reservoir study was conducted to determine the effects changing reservoir temperature would have on TOPAZ II if the cesium pressure throttle was not operating. Figure 26 illustrates how the system electric power and load voltage are affected by cesium reservoir temperature change.
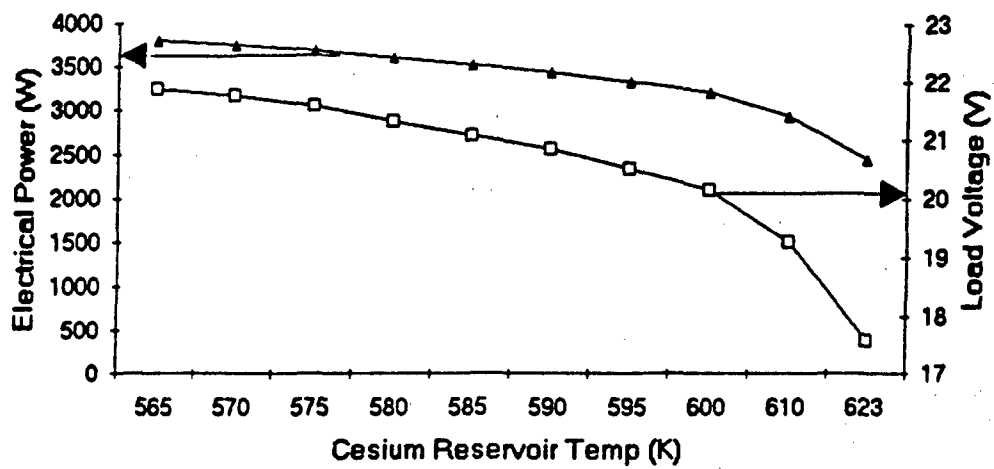
Figure 26. Cesium Reservoir Temperature Effect on Electrical Power and Load

Voltage

The results of the study indicates that the cesium reservoir temperature has a significant effect on system thermionic performance. The throttle is used to maintain a cesium vapor pressure of 2.0 torr. This corresponds to a reservoir temperature of approximately 580 K. If the throttle should fail and the normal cesium reservoir operating temperature of 623 K is maintained, the system power would drop by almost 30%.

How cesium reservoir temperature effects a thermionic diodes corresponding J-V curves was illustrated in Figure 5. Depending on what output voltage is desired, an optimum cesium pressure exists. As can be seen in Figure 5, small changes in reservoir temperature can cause significant changes in how efficiently a thermionic diode operates. To avoid power fluctuations due to small reservoir temperature deviations, the cesium reservoir temperature is often chosen to be higher than optimum(20: section 3). This explains the choice of 580 K for the design operating temperature.

The system efficiency becomes increasingly dependent on cesium reservoir temperature changes the further the temperature deviates from the design pressure. The results indicate a heavy reliance on the cesium reservoir throttle, as failure of it would cause a serious decrease in system efficiency. The results also cause questioning of the designers decision to operate the cesium r~ ;rvoir at such high temperatures.

V. Summary

Models based on the TDS thermionic diode model were developed for the TOPAZ
II and SPACE-R nuclear power systems. Due to computer code limitations inherent in the
TDS model, only the TOPAZ II system model ran successfully. Several parameter studies
were conducted on the TOPAZ II model. These studies determined system performance
and efficiency while varying the following:

1. The coolant flow inlet temperatures.

2. The rate of coolant temperature change.

3. The power profile of the core.

4. The cesium reservoir temperature.

Analysis of the results indicate that the model accurately represented the TOPAZ II
system, underestimating published data by 10%. Coolant flow parameter studies indicate
that raising coolant flow temperatures up to 100 K higher increases system power by up to
5%. Additional increases in temperature result in gradual performance degradation.
Varying the axial power profile of the core from the actual peaked profile to a flat profile
results in a negligible 0.3% change in total system performance. The peaked profile used
in TOPAZ II produces the highest system efficiency of all the profiles modeled. The
cesium pressure study indicates that the system is operating above optimum cesium
pressure and that system performance is strongly dependent on cesium pressure.
Increasing cesium reservoir temperature above design temperature by 30 K decreases
system efficiency by 30%.

Conclusions

The updated 'q_8_p' model is capable of conducting a variety of parameter studies on the TOPAZ II system. It is not yet capable of solving for the SPACE-R system as TDS cannot handle the parallel TFE circuitry arrangement used in SPACE-R. The 'q_8_p' model is a relatively straightforward tool for conducting parameter studies. It is limited in its ability to easily converge on a solution. Several parameter studies were limited by the parameter range for which the model can converge on a solution. The model specifically encountered significant difficulties when a TFE was operating in the unignited mode.

The parameter studies yield several conclusions. The system efficiency is not significantly affected by small excursions in coolant temperatures. In fact, system power increases by up to 6% for small increases in coolant inlet temperature. Not until the temperature was increased by approximately 100 K was the system adversely affected. After this point the system efficiency drops slowly for increased coolant temperatures.

Flattening the axial thermal profile in the power profile parameter study indicates that using axial reflectors and various fuel distribution techniques to smooth the axial power profile is not necessary. The most efficient power profile was actually the peaked normal profile used in the TOPAZ II design. The difference between its electrical power output and the power output of a completely flat axial thermal profile with the same total thermal power was less than 0.3%

A final conclusion is that the TOPAZ II cesium reservoir would not operate efficiently if the pressure throttle were to malfunction. A malfunction of the throttle under normal conditions would cause a decrease in electric power of almost 30%. This makes it a single point failure item in the overall system if full power is required.

Recommendations

Several problems that exist in TDS need to fixed before it can model a problem such as SPACE-R. This is due to circuitry modeling constraints inherent in TDS. For simple circuitry arrangements as that employed in TOPAZ II, TDS is an effective tool. Improvements in TDS can still be made   At present TDS requires a routine such as 'q_8_p' to help it build the system profile arrays and to assist it in converging on a solution. Much of 'q_8_p' should be included in the TDS code so that TDS can eventually achieve its advertised ability, the ability to interact in the GPS environment with other models such as coolant pumps and heat pipe radiators. Even then it may create problems as it often has difficulty converging on solutions. The TDS model is far from being a stand alone model which can be incorporated into a complete system model.

A possible use of TDS and 'q_8_p' could be to use them to build an extensive library of data tables which can be called on by a thermionic core model incorporated into a larger complete power system model. This would allow for a significantly faster routine with only limited degradation in accuracy. To build such data tables would require parameter studies such as those conducted for this paper, but on a broader and more extensive scale.

APPENDIX A: SPACE-R Modeling E

To model SPACE-R a very similar approach was taken as that used to model TOPAZ-II. The same basic TDS model setup was used as that described for TOPAZ II. The three things which had to be altered were the input system parameters, as outlined in Table 1; the core thermal profile; and the core configuration and wiring.

Most of the system parameters were found in the SPACE-R design study text (21). Several of the parameters such as contact and load resistance, collector work function, emitter emissivity, and most of the cesium vapor parameters were not given in the literature. The cesium vapor parameters were not given in the literature as the design team has not chosen the type of cesium reservoir system it will use. It can be assumed that whatever system they employ will provide cesium vapor in the gap at the optimum system pressure which can be solved for with the model. As the SPACE-R TFE collector and emitter materials are the same as those used for the TOPAZ II, collector work function and emitter emissivity were assumed to be the same. Load resistance was determined based on the desired system load voltage and the given current. Contact resistances were assumed to be the same as those in the TOPAZ II design.

Thermal profiles were obtained from SPACE-R design study results. The design study outlined both axial and radial thermal profiles for the SPACE-R core as shown in Figures 16 and 18. The radial profile was broken into four regions, A through D with the core center region being region A as shown on the bottom of Figure 16. An average thermal profile was determined for each region both axially and radially. Axially, the profile was split up depending on the number of nodes desired.

Modeling the electrical circuitry of SPACE-R with TDS was the most difficult task. The TFE's are not connected in series as in TOPAZ II. The TFE's are grouped

together into 37 small strings of 3 to 6 TFE's connected in parallel. These groups are then strung together in series to produce the desired 24 volts. Problems occur because TDS does not allow for an easy way to model different sized parallel strings connected in series.

The authors of TDS allowed for parallel and series connections of TFE's, but always assumed that such an arrangement would be symmetric; that is, they assumed all groups would be the same number of TFE's. TDS allows for grouping of TFE's into 'branches'. These branches are connected in series and TFE's in the branches are connected in series. Bus bars can additionally be introduced into the system between branches or inside branches in order to connect TFE's in parallel. To model the SPACE-R electrical circuitry required an indirect approach which utilized 'null' TFE's to be used.

The theory behind 'null' TFE's is that a TFE would have no affect on the system if it encountered: 1) no temperature differential between emitter and collector, 2) no heat flow across the inter-electrode gap, and 3) it had infinite resistance. This would allow SPACE-R to be modeled as a rectangular array with 37 branches of TFE's. Each branch would consist of six TFE's connected in parallel. The number of 'null' TFE's contained in each branch would be dependent on the number of TFE's each branch was really supposed to contain. Bus bars would be utilized in each branch so that TFE's connect in parallel.

Attempting to implement the full model of SPACE-R was broken into steps as GPS and TDS had never been used on such a large system before. Modeling techniques such as the 'null' TFE had also never been attempted before and needed to be tested. Below is a discussion of several of the models employed.

tdstest.dat

The first step in trying to model SPACE-R was to see if TDS could handle a system as large as that. A simple model was created which asked TDS to handle a 150 TFE core, connected in series, using three nodes per TFE, and with the thermal profile identical for

59

all 150 TFE's. This model is not a good simulation of the real system but allowed for the modeling of a large system that should easily converge on a solution.

The attempts to run 'tdstest.dat' showed that GPS needed to expand its array and vector dimensions in order to handle the problem as variable bounds were being exceeded. The authors of GPS made the necessary changes which allowed the model to run. The successful running of 'tdstest.dat' showed that GPS could handle a 150 TFE system, although the solutions obtained from it were not significant as the model was not accurate.

Test1.dat-Test3.dat

Three tests were designed to test if 'null' TFE's and multiple branches really worked. These tests were setup to run in the 'q_8_p' model discussed earlier. The object of the test was to prove that TDS yielded accurate results when modeling systems using 'null' TFE's and multiple branches. The system to be modeled was a simple 4 TFE system with each TFE having the same power profile. The three tests' electrical circuitry is diagrammed in Figure 27 below. The 'null' TFE is depicted by a darkened circle while the normal TFE's are depicted by empty circles.

a) Test1.dat   b) Test2.dat   c) Test3.dat
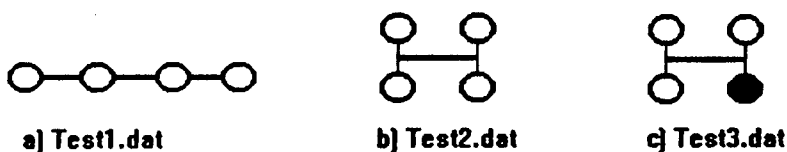
Figure 27. Wiring Schematic for Test1, Test2, & Test3.dat

In 'Test1.dat' the 4 TFEs are connected in series. This is a problem which has been shown by the authors to be analyzed correctly. It is a simple problem very similar to the TOPAZ II electrical setup, only smaller. The solutions from this test were to be used to compare with the results from the other tests.

60

In 'Test2.dat' the 4 TFE's were separated into two branches of 2 TFE's each. Additionally, each branch has one bus bar connection so that the TFE's in the branch are connected in parallel. The object of this was to show that TDS could handle parallel circuitry. Verification of the results would come from comparison to 'Test1.dat' results and simplified hand calculations checking to see if the circuit theory was correct.

In 'Test3.dat' one of the TFE's is replaced with a 'null' TFE. This 'null' TFE has infinite resistance with no thermal flow across the inter-electrode gap. The 'null' TFE will be moved around the array of 4 TFE's in order to test that the results are the same no matter were the 'null' TFE is found.

SPACER3.dat

In 'SPACER3.dat' the full SPACE-R reactor is modeled using 3 nodes per TFE. It is based on the 'q_8_p' model provided by Ralph Peters. Due to the wiring configuration discussed earlier, the core had no symmetry so the entire 150 TFE core had to be modeled. Collector temperatures were based on published coolant temperatures and the assumption that they were 25 K hotter than coolant temperatures. Thermal heat profiles were derived from Figures 16 and 18 as discussed earlier. Regions A through D were modeled separately and designated as regions 0 through 3. Each TFE was assigned the number which corresponded to the thermal region it was located in. Additionally, the null TFE was modeled as region 4. 37 separate branches were created with 6 TFE's per branch. Each branch had one bus bar connection thus linking the 6 TFE's in parallel. The entire system consisted of 37 bus bar connections and 222 TFE's. 72 of the TFE's were null TFE's however.

61

Results & Conclusions

Modification of GPS and TDS allowed 'tdstest.dat' to run successfully, showing that TDS can handle a system as large as SPACE-R dimensionally. TDS was unable to successfully converge on a solution, however, for a system which utilized parallel circuitry. No solution was ever achieved for Test2.dat and Test3.dat. The author of TDS, Ralph Peters, claims to have made the necessary changes to the model so that Test2.dat parallel circuitry now works. However, he could not get TDS to converge on a solution when 'null' TFE's were modeled. The CS model and the TECMDL both return reasonable solutions, but the routine which works to minimize the error between the two models has difficulty choosing new guesses for the iteration process.

With these problems still existing, the SPACER3.dat model was not even attempted as it is by far a more complex problem than the simple test problems.

To be able to model SPACE-R with TDS, several modifications are required. Either TDS has to be re-written to allow for the input of varying branch sizes or it has to modified so that 'null' TFE's can be introduced into the system without causing convergence complications. As 'null' TFE's were created to bypass model limitations, it would probably be best to change input format so that different branch sizes are allowed. This would allow TDS the flexibility it will require to model varied future TFE based power systems.

APPENDIX B: Updated 'q_8_p' TOPAZ II System Model

% This GPS code calculates the thermionic diode subsystem performance and

% the emitter temperature profile using as input the system design and

% properties, the thermal power input to the emitter, and the collector

% temperature profile.

%

% It is currently set up for TOPAZ II

%

% This calc. uses the fission power profiles from Eric Baker's 11/24/92 results.

% In this case, I explicitly put in the gap heat flows with a loop.

% 8 nodes per TFE with 34 TFEs in series

%

% np is in "tds" terminology, ntfe - the number of tfes in series

% REMEMBER! This code reads ./tds/tfe_sys.dat for much system information

% unless the "/file" parameter on the tds task statement is used.

% I am trying a sophisticated version of the "fixed point scheme" suggested

% by Howard Geyer on 9/11/92.

% Define the system components

/T_em_std { therm:

```
        /np  34 /nsrc 8 /t [100 100 100] } cdef


/T_col_std { therm:

      /np 34 /nsrc 8} cdef


/TI_del -1.e-5 def

/TI_acc 1.e-3 def

/TI_std { tds:

% Set up to use the local tfe_sys.dat file

    /file "./tfe_sys.dat"

    /acc TI_acc /length 0.375 /del TI_del /nsrc 8} cdef


% Read in the system definition from ./tds/tfe_sys.dat

  TI_std.in


% "ntot" is the total number of points in TFE ladder_array.

/ntot (TI_std.nsrc*TI_std.ntfe*TI_std.nbr) def


% Specify initial values of emitter temperatures

0 1 (ntot-1) {/i def /T_em_std.t[i] 1790. def} for


% Specify initial values of gap current

0 1 (ntot-1){/i def /TI_std.guess[i] 0.6 def} for


% Set init to 2 so that TI_std.guess is used as the initial value array

/TI_std.init 2 gdef
```

% Specify values of collector temperatures

0 T_col_std.nsrc (ntot-1){/i def /T_col_std.t[i] 781.0 def} for

1 T_col_std.nsrc (ntot-1){/i def /T_col_std.t[i] 794.0 def} for

2 T_col_std.nsrc (ntot-1){/i def /T_col_std.t[i] 806. def} for

3 T_col_std.nsrc (ntot-1){/i def /T_col_std.t[i] 819. def} for

4 T_col_std.nsrc (ntot-1){/i def /T_col_std.t[i] 831. def} for

5 T_col_std.nsrc (ntot-1){/i def /T_col_std.t[i] 844. def} for

6 T_col_std.nsrc (ntot-1){/i def /T_col_std.t[i] 856. def} for

7 T_col_std.nsrc (ntot-1){/i def /T_col_std.t[i] 869. def} for

% Set up specified heat profile - Based on Eric Baker's mcnp results!!

%   NOTE!! All arrays in this file are assumed to count the

%   way the "c" language counts, i.e., 0,1,2,3,..

%

%   nsrc is the number of sections that each TFE

%   divided into for computations (e.g., TI.nsrc)

%

%   NRGN is the number of axial profiles through the entire

%   reactor being used in computations.

%

%   nbr is the number of parallel branches of TFEs in the

%   ladder network (e.g., TI.nbr).

%

% NTS is the Number of TFEs in a "string". A "string" consists

% of all the TFEs in a single axial channel through the reactor. A

% "single cell" system, by definition has an NTS value of 1. Multi-cell

% systems have NTS values > 1.

%

% NS is the number of strings per branch. NS=ntfe/NTS

%

% shape_ax is the axial normalized power profile [0,1] of

% the reactor. The first set of "NTS*nsrc" points are for the

% first region which is usually the center of the reactor

% (maybe a single TFE), the second set of "NTS*nsrc" points are

% for the next region (usually the first ring around the central tfe),

% etc. until "NRGN" sets of axial profiles are specified. Array size is

% shape_ax[NRGN][NTS*nsrc] where the array is "rectangular"

% (e.g., shape_ax[i] has "NTS*nsrc" points for "i" in the range [0,NRGN-1]).

% The first point in an axial profile is assumed to be at the top or

% entrance to the reactor.

%

% q_peak is the peak value of the heat flux (w/cm2)from the fuel to the

% emitter. q_peak*shape_ax[i][j] gives the heat flux in the volume [i][j]

% tfe_rgn is the region number (see shape_ax above) for a string of

% TFEs (see NTS and NS above). The array is "rectangular" of size

% tfe_rgn[nbr][NS]. The first region number is "0", second region is "1"

% etc. in the manner that "c" and "gps" label array locations.

%

% dAsem is the area of a computational section of the emitter {cm2}.

% dAsem=(pi*demo*length*1.e4)/nsrc

%

% q_fl_em is the amount of heat passing into section "i" of the emitter in

% TFE number "j" of branch number "k". It is a rectangular array of size

% q_fl_em[nbr][ntfe][nsrc].

%

% q_fl_em[k][j][i]=dAsem*(shape_ax[tfe_rgn[k][j]][i])*q_peak

%

% See vardef.tfe for further explanation.

% TOPAZ II example - a "single-cell" design

/NRGN 4 sdef

/NTS 1 sdef

/NS (TI_std.ntfe/NTS) sdef

% Shapes from MCNP calcs by Eric Baker in November 1992

/shape_ax NRGN array sdef

% Actual normalized 8 node shapes from Eric - Regions 0 through 3

/shape_ax[0] [0.52873 0.74726 0.90925 0.98688 0.98688 0.90925 0.74726
0.52873] sdef

/shape_ax[1] [0.49217 0.67198 0.83294 0.91806 0.91806 0.83294 0.67198
0.49217] sdef

/shape_ax[2] [0.50605 0.71145 0.87550 0.96119 0.96119 0.87550 0.71145 0.50605] sdef

/shape_ax[3] [0.48486 0.68548 0.84026 0.91591 0.91591 0.84026 0.68548 0.48486] sdef

% 3 node shapes based on E Baker MCNP - not used for 8 node calculations

%/shape_ax[0] [0.70023 0.97592 0.70023] sdef

%/shape_ax[1] [0.64064 0.90509 0.64064] sdef

%/shape_ax[2] [0.67091 0.94892 0.67091] sdef

%/shape_ax[3] [0.64435 0.90620 0.64435] sdef

/q_peak 27. sdef

/tfe_rgn TI_std.nbr array sdef

% Based on "TOPAZ II Description - Top View Circuit Diagram" in TOPAZ CoDR

% Package from 9/16-17/92 meeting. Start with TFE #29 on diagram

/tfe_rgn[0] [3 3 3 3 3 3 3 2 2 2 2 2 2 2 2 2 2 1 1 1 1 0 1 1 2 2 3 3 3 3 3 3 3 3] sdef

/pi 3.14159265 sdef

% Area of a computational segment of the emitter

/dAsem ((pi*TI_std.demo*TI_std.length*1.e4)/TI_std.nsrc) sdef

% Print header for print in loop

%["\n k j i q_fl_em[k][j][i] shape_ax[(tfe_rgn[k][j])][i] tfe_rgn[k][j] "]printf

68

```
% Calculate q_fl_em

/q_fl_em TI_std.nbr array sdef


0 1 (TI_std.nbr-1) {/k sdef

        /q_fl_em[k] TI_std.ntfe array sdef

0 1 (TI_std.ntfe-1) {/j sdef

        /q_fl_em[k][j] TI_std.nsrc array sdef

0 1 (TI_std.nsrc-1) {/i sdef

        /q_fl_em[k][j][i]

            (dAsem*(shape_ax[(tfe_rgn[k][j])][i])*q_peak) sdef


% Print out values to check the computation

%["\n %.0f  %.0f %.0f %.3f  %.3f  %.0f" k j i q_fl_em[k][j][i]

shape_ax[(tfe_rgn[k][j])][i]  tfe_rgn[k][j] ] printf



        } for

        } for

        } for


% This completes calculations concerning the heat flow into the emitter.

%

%

% The next major segment sets up variables, arrays, etc. needed to control the

% iteration.
```

69

```
%

% Heat error array -- current pass -- is q_er

/q_er    TI_std.nbr array sdef


% Heat error array -- previous pass -- is q_er_old

/q_er_old TI_std.nbr array sdef


% delta in emitter temperature over the last iteration.

/del_T    TI_std.nbr array sdef


% A large loop to set these 3 arrays up.

0 1 (TI_std.nbr-1) {/k sdef

        /q_er[k]     TI_std.ntfe array sdef

        /q_er_old[k] TI_std.ntfe array sdef

        /del_T[k]    TI_std.ntfe array sdef

0 1 (TI_std.ntfe-1) {/j sdef

        /q_er[k][j]     TI_std.nsrc array sdef

        /q_er_old[k][j] TI_std.nsrc array sdef

        /del_T[k][j]    TI_std.nsrc array sdef

0 1 (TI_std.nsrc-1) {/i sdef

        /q_er[k][j][i]  10. sdef

        /del_T[k][j][i] 0 sdef

        } for

        } for

        } for
```

```
% T_em_old is the emitter temperature array that holds the results of the last
% successful calculation.  It is used if the code needs to step back to a
% point near a successful calculation.
/T_em_old ntot array sdef
0 1 (ntot-1) {/l def /T_em_old[l] T_em_std.t[l] gdef} for


% Arrays of different ages of guesses - Needed for the backstep
/G_old ntot array sdef
/G_cur ntot array sdef
0 1 (ntot-1){ /i def /G_old[i] TI_std.guess[i] gdef
            /G_cur[i] TI_std.guess[i] gdef} for


% Error tolerance where the error is average RMS error normalized by the
% heat crossing the gap at each point.
/q_acc 1.e-5 def


% Specify what fraction of "step" to take, ep_mul <=.5
/ep_mul .35 def
% Minimum ep_mul, then an interupt in gps script
/ep_mul_min 1.e-6 def


% Specify how much to change ep_mul, delTmax_u, and delTmin_u
% (by multiplying by "step_use") if they are too large.  "step_ch"
% reduces the size of step_use.
/step_ch .1 def
/step_use 1. gdef
```

% Max and min limits on epf ({delta Temperature}/{delta q error} for a step

/epfmax (.1*dAsem) sdef

/epfmin (3.e-3*dAsem) sdef

% Max and min changes on emitter temperature - currently not used,

% so set to a large value.

/delTmax 100. sdef

/delTmin -100. sdef

/delTmax_u delTmax def

/delTmin_u delTmin def

%. Bounds on the maximum error in the tds calculation for a particular

% emitter temperature profile. If fofx is bigger than "fofxbnd_u"

% then many parameters (e.g., ep_mul_u, are reduced in size) to reduce

% step size for the next iteration.

/fofxbnd_u .2 def

/fofxbnd_l (fofxbnd_u/15.) def

% Temporary initializations

%epf is the ratio "del_T / (q_er_old - q_er)" for last step

/epf ntot array sdef

0 1 (ntot-1){/i def /epf[i] (1.01*epfmin) def} for

```
/dq 2.7 sdef

/q_peak (q_peak+dq) gdef


% START OF HUGE "FOR" LOOP on q_peak


0 1 0 {

/q_peak (q_peak-dq) gdef

/TI_std.acc TI_acc gdef

% Set the starting value fo ep_mul_u used a little smaller; it can grow as large

% as ep_mul if the solutions are "easy"

/ep_mul_u (ep_mul/3.) def

% Recalculate q_fl_em, etc....

0 1 (TI_std.nbr-1)  {/k sdef

0 1 (TI_std.ntfe-1) {/j sdef

0 1 (TI_std.nsrc-1) {/i sdef

        /q_fl_em[k][j][i]

            (dAsem*(shape_ax[((tfe_rgn[k][j])][i])*q_r)ak) gdef

        /q_er[k][j][i]  10. gdef

        /del_T[k][j][i] 0 gdef


0 1 (ntot-1){ /i def /G_old[i] TI_std.guess[i] gdef

            /G_cur[i] TI_std.guess[i] gdef

            /epf[i] (1.01*epfmin)    gdef} for
```

73

% Print out values to check the computation

%["\n %.0f %.0f %.0f %.3f %.3f %.0f" k j i q_fl_em[k][j][i]

shape_ax[((tfe_rgn[k][j])]][i] tfe_rgn[k][j]] printf


```
            } for
            } for
            } for
```


% Temporary initialization of thermal power

/TI_std.pt 1 def

% Loop counter

/iwhile 0 sdef

% Step flag - how many small steps the code must take before going

% back toward the input step size, etc. after making a backward step.

/step 10 sdef

/stpc -1 sdef

%

%

%

% START OF CALCULATION - It is in the form of (cond) {calc} while

```
%

% CONSTRAINT that trys to set q_er_t to zero in a "while" loop

{ /q_er_t 0.0 sdef

 /q_er_t_sr 100.0 sdef

  (iwhiie > 0) {

% Calculate Normalized mean squared heat error - q_er_t

0 1 (TI_std.nbr-1) {/k sdef

0 1 (TI_std.ntfe-1) {/j sdef

0 1 (TI_std.nsrc-1) {/i sdef

        /l (TI_std.ntfe*TI_std.nsrc*k+TI_std.nsrc*j+i) sdef

        /den (q_fl_em[k][j][i]+TI_std.qoem[l]) sdef

        /q_er_t (q_er_t + (q_er[k][j][i]*q_er[k][j][i])/(den*den)) gdef

        } for

        } for

        } for


% Divide q_er_t by ntot and find square root

 /q_er_t_sr (pow((q_er_t/ntot),0.5)) gdef


% Reset TI_std.acc as q_er_t_sr gets small

  (q_er_t_sr < (TI_std.acc*20.) ){/TI_std.acc (max(5.e-7,(TI_std.acc /10.))) gdef}if


% Print Normalized RMS error and other relevant information

["\n iwhile= %.0f  NORMALIZED Avg. thermal error = %.4e" iwhile

q_er_t_sr]printf
```

```
    ["\n q_er_t_sr = %.3e q_acc = %.3e ep_mul_u = %.3e  TI_std.acc = %.3e "

q_er_t_sr q_acc ep_mul_u TI_std.acc ]printf

    ["\n  TI_std.fofxmax = %.4e" TI_std.fofxmax]printf

    } if

    %  Is the calculation done?

      (q_er_t_sr > q_acc)

    }

    % Now the "calc" portion


    {


      % Use tasks to calculate tds performance

        T_col_std.c

        TI_std.s

        T_em_std.c

        TI_std.c

      % Optional printouts for HELP

      0 1 (TI_std.nbr-1)  {/k sdef

      1 8 (TI_std.ntfe-1) {/j sdef

      0 1 (TI_std.nsrc-1) {/i sdef

            /l (TI_std.ntfe*TI_std.nsrc*k+TI_std.nsrc*j+i) sdef

        ["\n %.0f %.0f %.0f %.0f %.3f %.3f %.3f %.3f %.3f   %.3f %.3f %.9f %.9f %.3f"

k j i l q_fl_em[k][j][i] TI_std.qoem[l] q_er[k][j][i] del_T[k][j][i] epf[l] T_em_std.t[l]

TI_std.vgap[l]  TI_std.igap[l] TI_std.guess[l] TI_std.flco.q[l]]printf

            } for

            } for
```

```
        } for


% Update T_em, GUESS if the solution is valid!


(TI_std.fofx < TI_std.acc)

{

% Reduce counter used if a "backstep" occurs
/stpc (stpc-1) gdef


% Reset a number of parameters if the code has had
% no problems.
/step_use 1. gdef
%
% Change ep_mul_u based on largest fofx in last calculation
((TI_std.fofxmax < fofxbnd_l) && (stpc < 0) && (iwhile > 2))
{/ep_mul_u  (min(ep_mul,(ep_mul_u*2.0))) gdef
 /delTmax_u (min(delTmax,(delTmax_u*2.0))) gdef
 /delTmin_u (max(delTmin,(delTmin_u*2.0))) gdef
 /TI_std.del TI_del gdef} if


((TI_std.fofxmax > fofxbnd_u) && (iwhile > 0))
{/ep_mul_u (ep_mul_u/4.) gdef
 /delTmax_u (delTmax_u/4.) gdef
 /delTmin_u (delTmin_u/4.) gdef } if


% Roll the guesses into their appropriate arrays
```

77

```
0 1 (ntot-1){ /i def /G_old[i] G_cur[i] gdef
              /G_cur[i] TI_std.guess[i] gdef} for


% Calc. new temps,etc
0 1 (TI_std.nbr-1)  {/k sdef
0 1 (TI_std.ntfe-1) {/j sdef
0 1 (TI_std.nsrc-1) {/i sdef

        /l (TI_std.ntfe*TI_std.nsrc*k+TI_std.nsrc*j+i) sdef

        /q_er_old[k][j][i] q_er[k][j][i] gdef

        /q_er[k][j][i] (q_fl_em[k][j][i]+TI_std.qoem[l] -

              TI_std.flco.q[l]) gdef



% Save T_em if the code needs to back-step.
        /T_em_old[l] T_em_std.t[l] gdef


% Calculate epf array
        (iwhile > 0){ /epf[l]  (max(epfmin,(min(epfmax,(.90*epf[l]+.10*

        (del_T[k][j][i]/(q_er_old[k][j][i]

         -q_er[k][j][i])))))))) def} if


% Calculate del_T array  ·
        /del_T[k][j][i]

   (max(delTmin_u,(min(delTmax_u,(ep_mul_u*epf[l]*q_er[k][j][i]))))) def


% Calculate next T_em array
```

78

```
        /T_em_std.t[l] (T_em_std.t[l] + del_T[k][j][i]) def


    % Optional printout for HELP

    %["\n %.0f %.0f %.0f %.0f  %.3f %.3f %.3f " k j i l del_T[k][j][i] epf[l]
T_em_std.t[l] ]printf

                } for

                } for

                } for


        }


    % "backstep" portion


    {
    ["\n tds task did not find a solution,"]printf

    ["\n take a smaller step from old loc."]printf

    % If the solution is not valid, move T_em back toward the previous location,

    % set init to 2 so that guess is read in for a recalculation, and decrease

    % ep_mul_u, delTmax_u, and delTmin_u

    (stpc == step) {["No solution on the backstep"]printf sintrp} if


    /ep_mul_u (ep_mul_u*step_ch) gdef

    /delTmax_u (delTmax_u*step_ch) gdef

    /delTmin_u (delTmin_u*step_ch) gdef

    /step_use (step_use*step_ch) gdef

    /TI_std.init 2 gdef
```

% Reset "del" to force the jacobian to be calculated every time tds

% starts a new calculation.

(TI_std.del < 0.0) {/TI_std.del (-TI_std.del) gdef } if

% Move a back to the old location and redo that calculation

0 1 (TI_std.nbr-1) {/k sdef

0 1 (TI_std.ntfe-1) {/j sdef

0 1 (TI_std.nsrc-1) {/i sdef

        /l (TI_std.ntfe*TI_std.nsrc*k+TI_std.nsrc*j+i) sdef

        /T_em_std.t[l] (T_em_old[l]) def

%   /T_em_std.t[l] (T_em_old[l] + del_T[k][j][i]* step_use) def

% Set TI_std.guess to the guess that gave rise

% to the last successful calculation

% Trying G_cur again

            /TI_std.guess[l] G_cur[l]gdef

% Optional printout for HELP

["\n %.0f %.0f %.0f %.0f %.3f %.3f %.3f " k j i l del_T[k][j][i] epf[l]

T_em_std.t[l]]printf

            } for

            } for

            } for

% Optional printouts for HELP

80

```
["\n ep_mul_u =%.3e init= %.0f" ep_mul_u TI_std.init]printf
0 1 (ntot-1) {/m def ["\n m= %.0f guess=%.3e" m TI_std.guess[m]
]printf}for


% Set stpc equal to step to keep step sizes small for a while
/stpc step gdef


} ifelse


(ep_mul_u <= ep_mul_min){
            ["\n\n ep_mul_u = %.3e  ep_mul_min = %.3e " ep_mul_u
ep_mul_min]printf
            ["\n If you type resume, then ep_mul_min is reduced by 10"]printf
            ["\n and the calculation continues"]
            sintrp
            /ep_mul_min (ep_mul_min/10.) gdef


    }if


/iwhile (iwhile+1.) gdef
}while


% This is the end of the "(cond) {calc} while" loop
%
% PRINTOUT Results
["\n RESULTS  q_peak= %.3f\n" q_peak]printf
```

```
TI_std.out

mods.print

therms.print

TI_std.print


%  Printout stuff for plotting


["\n \n data for plotting  q_peak = %.4f\n" q_peak]printf

["\n k j i l q_fl_em[] TI_std.qoem[] T_em_std.t[] TI_std.vgap[]  TI_std.igap[]
TI_std.flco.q[]"]printf


0 1 (TI_std.nbr-1)  {/k sdef

0 1 (TI_std.ntfe-1) {/j sdef

0 1 (TI_std.nsrc-1) {/i sdef

        /l (TI_std.ntfe*TI_std.nsrc*k+TI_std.nsrc*j+i) sdef

   ["\n %.0f %.0f %.0f %.0f %.3f %.3f %.3f %.3f %.3f %.3f" k j i l q_fl_em[k][j][i]
TI_std.qoem[l] T_em_std.t[l] TI_std.vgap[l]  TI_std.igap[l] TI_std.flco.q[l]]printf

        } for

        } for

        } for

% DONE!


} for

% This is the end
```

APPENDIX C: Sample 'q_3_p' Output (The 3 node version of 'q_8_p')

RESULTS for q_peak= 27.000

output of model parameters

T_em_std   np=34 nsrc=3 nin=102 heat=0.000e+00

t=1882.9 2037.8 1886.4 1882.8

2037.8 1886.4 1882.8 2037.8 1886.4

1882.8 2037.8 1886.4 1882.8 2037.8

1886.4 1882.8 2037.8 1886.4 1882.8

2037.8 1886.4 1902.3 2068.4 1905.8

1902.3 2068.4 1905.8 1902.3 2068.4

1905.8 1902.3 2068.4 1905.8 1902.3

2068.4 1905.8 1902.3 2068.4 1905.8

1902.3 2068.4 1905.8 1902.3 2068.4

1905.8 1902.3 2068.4 1905.8 1902.3

2068.4 1905.8 1880.1 2036.5 1883.8

"Emmitter Temperature profile wher 'np' signifies the

number of TFE's, 'nsrc' is the number of nodes, and 'nin'

is the total array size. 't' represents the array of

temperatures . The first value represents the emitter

temp of the first TFE's first node. The second value

represents the second node of the first TFE, etc...

The array ends with the last TFE's last node emitter temp.

83

1880.1 2036.5 1883.8 1880.1 2036.5

1883.8 1880.1 2036.5 1883.8 1923.0

2088.7 1926.4 1880.1 2036.5 1883.8

1880.1 2036.5 1883.8 1902.3 2068.4

1905.8 1902.3 2068.4 1905.8 1882.8

2037.8 1886.4 1882.8 2037.8 1886.4

1882.8 2037.8 1886.4 1882.8 2037.8

1886.4 1882.8 2037.8 1886.4 1882.8

2037.8 1886.4 1882.8 2037.8 1886.4

1882.7 2037.8 1886.5

T_col_std   np=34 nsrc=3 nin=102 heat=0.000e+00

t=794.0 831.0 856.0 794.0

831.0 856.0 794.0 831.0 856.0

794.0 831.0 856.0 794.0 831.0

856.0 794.0 831.0 856.0 794.0

831.0 856.0 794.0 831.0 856.0

794.0 831.0 856.0 794.0 831.0

856.0 794.0 831.0 856.0 794.0

"The same as above except for the collector temperature array"

831.0 856.0 794.0 831.0 856.0

794.0 831.0 856.0 794.0 831.0

856.0 794.0 831.0 856.0 794.0

831.0 856.0 794.0 831.0 856.0

794.0 831.0 856.0 794.0 851.0

856.0 794.0 831.0 856.0 794.0

831.0 856.0 794.0 831.0 856.0

794.0 831.0 856.0 794.0 831.0

856.0 794.0 831.0 856.0 794.0

831.0 856.0 794.0 831.0 856.0

794.0 831.0 856.0 794.0 831.0

855.0 794.0 831.0 856.0 794.0

831.0 856.0 794.0 831.0 856.0

794.0 831.0 856.0

output of model therm flows

85

Average Collector Temps

T_col_std   np=34 nsrc=3 heat=0.000e+00

np= 0   t= 794.00 831.00 856.00   q= 0.000e+00 0.000e+00 0.000e+00

Average Emitter Temps

T_em_std   np=34 nsrc=3 heat=0.000e+00

np= 0   t=1882.87 2037.80 1886.36   q= 0.000e+00 0.000e+00 0.000e+00

System Parameters in TDS

TI_std   np=34 nsrc=3 heat=1.585e+05

np= 0   t= 794.00 831.00 856.00   q= 1.348e+03 1.886e+03 1.348e+03

TI_std   pload=6.9693e+03 vload=2.9632e+01 gload=7.9375e+00 clf=4.4181e-02

itot=2.3520e+02 p=8.3323e+03 preac=1.5775e+05

isolidem=12 isolidcr=13

ntfe=34 nsrc=3 init=0 isolv=1 iemphi=0

phi0=4.9500e+00 phicr=1.7000e+00 epsem=2.0000e-01

tr=5.8000e+02 trdes=600.00 601.00 prdcs=3.550 3.560

demi=1.7300e-02 demo=1.9600e-02 dcri=2.0600e-02 dcro=2.3400e-02

length=3.7500e-01

data for plotting q_peak = 27.0000

Position	Emitter Current	Emitter Current Density	Gap Temp	Gap Current Voltage	Collector Current	Current
k j i l	q_fl_em[]	TI_std.qoem[]	T_em_std.t[]	TI_std.vgap[]	TI_std.igap[]	TI_std.flco.q[]
0 0 0 0	1339.065	9.021	1882.866	0.997	0.844	1348.084
0 0 1 1	1883.232	3.038	2037.799	1.070	1.332	1886.248
0 0 2 2	1339.065	9.147	1886.361	0.999	0.880	1348.209
0 1 0 3	1339.065	9.085	1882.798	0.997	0.845	1348.148
0 1 1 4	1883.232	.038	2037.798	1.070	1.332	1886.249
0 1 2 5	1339.065	9.083	1886.429	0.999	0.879	1348.145
0 2 0 6	1339.065	9.087	1882.797	0.997	0.845	1348.150
0 2 1 7	1883.232	3.038	2037.798	1.070	1.332	1886.249
0 2 2 8	1339.065	9.081	1886.430	0.999	0.879	1348.143
0 3 0 9	1339.065	9.087	1882.797	0.997	0.845	1348.150
0 3 1 10	1883.232	3.038	2037.798	1.070	1.332	1886.249
0 3 2 11	1339.065	9.081	1886.430	0.999	0.879	1348.143
0 4 0 12	1339.065	9.087	1882.797	0.997	0.845	1348.150
0 4 1 13	1883.232	3.038	2037.798	1.070	1.332	1886.249
0 4 2 14	1339.065	9.081	1886.430	0.999	0.879	1348.143
0 5 0 15	1339.065	9.087	1882.797	0.997	0.845	1348.150
0 5 1 16	1883.232	3.038	2037.798	1.070	1.332	1886.249

87

0 5 2 17	1339.065	9.081	1886.430	0.999	0.879	1348.143
0 6 0 18	1339.065	9.087	1882.797	0.997	0.845	1348.150
0 6 1 19	1883.232	3.038	2037.798	1.070	1.332	1886.249
0 6 2 20	1339.065	9.081 1	886.431	0.999	0.879	1348.143
0 7 0 21	1394.261	9.119	1902.291	1.031	0.867	1403.376
0 7 1 22	1972.011	2.890	2068.414	1.103	1.288	1974.879
0 7 2 23	1394.261	9.118	1905.840	1.033	0.901	1403.374
0 8 0 24	1394.261	9.119	1902.292	1.031	0.867	1403.375
0 8 1 25	1972.011	2.890	2068.414	1.103	1.288	1974.879
0 8 2 26	1394.261	9.118	1905.840	1.033	0.901	1403.374
0 9 0 27	1394.261	9.119	1902.292	1.031	0.867	1403.375
0 9 1 28	1972.011	2.890	2068.414	1.103	1.288	1974.879
0 9 2 29	1394.261	9.118	1905.840	1.033	0.901	1403.374
0 10 0 30	1394.261	9.119	1902.292	1.031	0.867	1403.375
0 10 1 31	1972.011	2.890	2068.414	1.103	1.288	1974.879
0 10 2 32	1394.261	9.118	1905.840	1.033	0.901	1403.374
0 11 0 33	1394.261	9.119	1902.292	1.031	0.867	1403.375

0 11 1 34	1972.011	2.890	2068.414	1.103	1.288	1974.879
0 11 2 35	1394.261	9.118	1905.840	1.033	0.901	1403.374
0 12 0 36	1394.261	9.119	1902.292	1.031	0.867	1403.375
0 12 1 37	1972.011	2.890	2068.414	1.103	1.288	1974.879
0 12 2 38	1394.261	9.118	1905.840	1.033	0.901	1403.374
0 13 0 39	1394.261	9.119	1 902.292	1.031	0.867	1403.375
0 13 1 40	1972.011	2.890	2068.414	1.103	1.288	1974.879
0 13 2 41	1394.261	9.118	1905.840	1.033	0.901	1403.374
0 14 0 42	1394.261	9.119 1	902.292	1.031	.867	1403.375
0 14 1 43	1972.011	2.890	2068.414	1.103	1.288	1974.879
0 14 2 44	1394.261	9.118	1905.840	1.033	0.901	1403.374
0 15 0 45	1394.261	9.119	1902.292	1.031	0.867	1403.375
0 15 1 46 1	972.011	2.890	2068.414	1.103	1.288	1974.879
0 15 2 47	1394.261	9.118	1905.840	1.033	0.901	1403.374

016 0 48	1394.261	9.119	1902.292	1.031	0.867	1403.375
016 1 49	1972.011	2.890	2068.414	1.103	1.288	1974.879
016 2 50	1394.261	9.118	1905.840	1.033	0.901	1403.374
017 0 51	1331.355	9.090	1880.136	0.992	0.840	1340.443
017 1 52	880.925	3.073	2036.498	1.065	1.341	1883.977
017 2 53	1331.355	9.084	1883.783	0.994	0.875	1340.437
018 0 54	1331.355	9.090	1880.136	0.992	0.840	1340.444
018 1 55	1880.925	3.073	2036.498	1.065	1.341	1883.977
018 2 56	1331.355	9.084	1883.784	0.994	0.875	1340.436
019 0 57	1331.355	9.090	1880.136	0.992	0.840	1340.444
019 1 58	1880.925	3.073	2036.498	1.065	1.341	1883.978
019 2 59	1331.355	9.084	1883.784	0.994	0.875	1340.436
020 0 60	1331.355	9.090	1880.135	0.992	0.840	1340.443
020 1 61	1880.925	3.073	2036.498	1.065	1.341	1883.977
020 2 62	1331.355	9.084	1883.784	0.994	0.875	1340.436

021063	1455.192	9.135	1922.986	1.068	0.894	1464.327
021164	2028.121	2.697	2088.6?	1.137	1.235	2030.815
021265	1455.192	9.139	1926.443	1.070	0.927	1464.331
022066	1331.355	9.090	1880.132	0.992	0.840	1340.424
022167	1880.925	3.073	2036.483	1.065	1.341	1883.906
022268	1331.355	9.084	1883.781	0.994	0.875	1340.436
023069	1331.355	9.090	1880.135	0.992	0.840	1340.439
023170	1880.925	3.074	2036.497	1.065	1.341	1883.975
023271	1331.355	9.084	1883.783	0.994	0.875	1340.432
024072	1394.261	9.119	1902.291	1.031	0.867	1403.376
024173	1972.011	2.890	2068.414	1.103	1.288	1974.879
024274	1394.261	9.117	1905.840	1.033	0.901	1403.374
025075	1394.261	9.119	1902.292	1.031	0.867	1403.375
025176	1972.011	2.890	2068.414	1.103	1.288	1974.879

91

ID						
0 25 2 77	1394.261	9.118	1905.840	1.033	0.901	1403.374
0 26 0 78	1339.065	9.087	1882.797	0.997	0.845	1348.149
0 26 1 79	1883.232	3.038	2037.798	1.070	.332	1886.249
0 26 2 80	1339.065	9.082	1886.430	0.999	0.879	1348.144
0 27 0 81	1339.065	9.087	1882.797	0.997	0.845	1348.150
0 27 1 82	1883.232	3.038	2037.798	1.070	1.332	1886.249
0 27 2 83	1339.065	9.081	1886.430	0.999	0.879	1348.143
0 28 0 84	1339.065	9.087	1882.797	0.997	0.845	1348.150
0 28 1 85	1883.232	3.038	2037.798	.070	1.332	1886.249
0 28 2 86	1339.065	9.081	1886.430	0.999	0.879	1348.143
0 29 0 87	1339.065	9.087	1882.797	0.997	0.845	1348.150
0 29 1 88	1883.232	3.038	2037.798	1.070	1.332	1886.249
0 29 2 89	1339.065	9.081	1886.430	0.999	0.879	1348.143
0 30 0 90	1339.065	9.087	1882.797	0.997	0.845	1348.150

92

03 01 91	1883.232	3.038	2037.798	1.070	1.332	1886.249
03 02 92	1339.065	9.081	1886.430	0.999	0.879	1348.143
03 10 93	1339.065	9.087	1882.797	0.997	0.845	1348.150
03 11 94	1883.232	3.038	2037.798	1.070	1.332	1886.249
03 12 95	1339.065	9.081	1886.431	0.999	0.879	1348.143
03 20 96	1339.065	9.087	1882.795	0.997	0.845	1348.150
03 21 97	1883.232	3.038	2037.798	1.070	1.332	1886.249
03 22 98	1339.065	9.081	1886.432	0.999	0.879	1348.143
03 30 99	1339.065	9.088	1882.737;	0.996	0.845	1348.151
03 31 100	1883.232	3.038	2037.797	1.070	1.332	1886.249
03 32 101	1339.065	9.080	1886.490	0.999	0.878	1348.142

BIBLIOGRAPHY

1. Baker, Eric. "MCNP Study of TOPAZ II Nuclear Profile." Personal Correspondence. PL/VTP, Kirtland AFB, NM, 24 November 1992.

2. Bennett, Gary L. and A. Dan Schnyer. "Nasa Mission Planning for Space Nuclear Power." Proceedings of the AIP 8th Annual Symposium on Space Nuclear Power Systems. 77-82. New York: AIP Press, 1991.

3. Dorf-Gorsky, I. A. et al. "Cesium Feeder for the TOPAZ II System Study Results and Service Life Characteristics." Proceedings of the AIP 9th Annual Symposium on Space Nuclear Power Systems. 35-40. New York: AIP Press, 1992.

4. El-Genk, Mohammed S. et al. ""TITAM" Thermionic Integrated Transient Analysis Model: Load Following of a Single-Cell TFE". Proceedings of the AIP 9th Annual Symposium on Space Nuclear Power Systems. 1013-1022. New York: AIP Press, 1992.

5. ----------. "A Transient Model for a Cesium Vapor Thermionic Converter." Proceedings of the AIP 9th Annual Symposium on Space Nuclear Power Systems. 1259-1264. New York: AIP Press, 1991.

6. Flight Safety Team, U.S. Topaz II. NEP Space Test Program Preliminary Nuclear Safety Assessment. November 1992.

7. Geyer, H.K. GPS- A PostScript-like Language for System Simulations. Engineering Physics Division, Argonne National Laboratory, Illinois, April 1992.

8. ----------. GPS/Model Interfacing. Engineering Physics Division, Argonne National Laboratory, Illinois, April 1992.

9. ----------. GPSTool User's Manual. Engineering Physics Division, Argonne National Laboratory, Illinois, April 1992.

94

10. Gryaznov, Georgy et al. "Cesium Vapor Supply System for TOPAZ SNPS." Proceedings of the AIP 9th Annual Symposium on Space Nuclear Power Systems. 58a-58g. New York: AIP Press, 1992.

11. Hatsopoulos, G.N. and E.P. Gyftopoulos. Thermionic Energy Conversion, Volume I. Cambridge, Mass: MIT Press, 1973.

12. Lamp, Tom and Brian Donovan. "Advanced Thermionics Technology Programs at Wright Laboratory." Proceedings of the AIP 9th Annual Symposium on Space Nuclear Power Systems. 617-622. New York: AIP Press, 1992.

13. Mills, Joseph C. and Richard Dahlberg. "Thermionic Systems for DOD Missions." Proceedings of the AIP 8th Annual Symposium on Space Nuclear Power Systems. 1088-1092. New York: AIP Press, 1992.

14. Nichols, Capt Don F. Modeling of and Investigation of Thermionic Diodes and Triodes. PhD Prospectus. School of Engineering, Air Force Institute of Technology (AU), Wright-Patterson AFB OH, October 1992.

15. Nicitin, V.P. et al. "Special Features and Results of the TOPAZ II Nuclear Power System Tests with Electrical Heating." Proceedings of the AIP 9th Annual Symposium on Space Nuclear Power Systems. 41-46. New York: AIP Press, 1992.

16. Pawlowski, Ronald and Andrew C. Klein. "Modeling the Energy Transport Through a Thermionic Fuel Element". Proceedings of the AIP 9th Annual Symposium on Space Nuclear Power Systems. 1123-1128. New York: AIP Press, 1992.

17. Peters, Ralph R. and Todd B. Jekel. "Thermionic Diode Subsystem Model". Proceedings of the AIP 9th Annual Symposium on Space Nuclear Power Systems. 1114-1122. New York: AIP Press, 1992.

18. Peters, Ralph R. "q_8_p." Computer Code given in Personal Correspondence. PL/VTP, Kirtland AFB, NM, October 1992.

95

19. Program Staff, Space Power Inc. "SPACE-R Thermionic Space Nuclear Power System Design Study, Draft Final Report." Report under contract F29601-90-C-0048 to the Air Force Space Technology Center, Phillips Laboratory, Kirtland AFB NM, October 1991.

20. Rasor, Ned S. Applied Atomic Collision Phsysics, Volume 5, Chapter 5: "Thermionic Energy Conversion," Edited by H. Massey, E. McDaniel, and B. Bederson. Academic Press, 1982.

21. ----------. "Thermionic Energy Conversion." A Short Course. Sunnyvale, California: Rasor Associates, Inc., September 1991.

22. Rhee, Hyop S. et al. "SPACE-R Thermionic Space Nuclear Power System with Single Cell Incore Thermionic Fuel Elements". Proceedings of the AIP 9th Annual Symposium on Space Nuclear Power Systems. 120-129. New York: AIP Press, 1992.

23. TECMDL: Ignited Mode Planar Thermionic Converter Model. Sunnyvale, California:Rasor Associates, Inc., August 1990.

24. UNIG: Unignited Mode Thermionic Converter Model. Sunnyvale, California:Rasor Associates, Inc., January 1991.

25. Van Hagan, Thomas H. et al. "TFE Fast Driver-Reactor System for Low-Power Applications." Proceedings of the AIP 9th Annual Symposium on Space Nuclear Power Systems. 498-503. New York: AIP Press, 1992.

Vita

First Lieutenant Otto D. Habedank was born on 21 April 1968 in Minot, North Dakota. He graduated from Alconbury High School in Alconbury, England in 1986 and attended the U S. Air Force Academy. He graduated with a Bachelor of Science in Physics in May 1990. Upon graduation, he received a regular commission in the U.S. Air Force and spent his first tour attending Undergraduate Pilot Training (UPT) at Williams AFB, Arizona. He graduated from UPT in July 1991, and under the Air Force's banked pilot system entered the School of Engineering, Air Force Institute of Technology, in August 1991.

Permanent Address: Lt. Otto D. Habedank

Box 6399 E. Turkey Trail

Hernando, FL 32642-2421

REPORT DOCUMENTATION PAGE

1. AGENCY USE ONLY (Leave blank)	2. REPORT DATE March 1993	3. REPORT TYPE AND DATES COVERED Master's Thesis

4. TITLE AND SUBTITLE Analysis of TOPAZ II and SPACE-R Space Nuclear Power Plants Using a Modified Thermionic Model	5. FUNDING NUMBERS
6. AUTHOR(S) Otto D. Habedank, 1Lt, USAF	
7. PERFORMING ORGANIZATION NAME(S) AND ADDRESS(ES) Air Force Institute of Technology, WPAFB OH 45433-6853	8. PERFORMING ORGANIZATION REPORT NUMBER AFIT/GNE/ENP/93M-03
9. SPONSORING/MONITORING AGENCY NAME(S) AND ADDRESS(ES) Capt Mark Dibben PL/VTP Kirtland AFB, NM 87117	10. SPONSORING/MONITORING AGENCY REPORT NUMBER

11. SUPPLEMENTARY NOTES

12a. DISTRIBUTION/AVAILABILITY STATEMENT Approved for public release; distribution unlimited	12b. DISTRIBUTION CODE

13. ABSTRACT (Maximum 200 words)

Models based on the TDS thermionic diode model were developed for TOPAZ II and SPACE-R nuclear power systems. Several parameter studies were conducted with the TOPAZ II model. These determined system performance and efficiency while varying the following: (1.) Coolant flow inlet temperatures. (2.) Rate of coolant temperature change. (3.) Power profile of the core. (4.) Cesium reservoir temperature. Analysis of results indicate the model accurately represented the TOPAZ II system, underestimating published data by 10%. Coolant flow studies indicate that raising coolant temperatures up to 100 K higher increases system power by up to 5%. Additional increases in temperature result in gradual performance degradation. Varying the axial power profile of the core from the actual peaked profile to a flat profile results in a negligible 0.3% change in system performance. The peaked profile used in TOPAZ II produces the highest system efficiency of all the profiles modeled. The cesium pressure study indicates the system is operating above optimum cesium pressure and system performance is strongly dependent on cesium pressure. Increasing cesium reservoir temperature above design temperature by 30 K decreases system efficiency by 30%.

14. SUBJECT TERMS Space Nuclear Power, TOPAZ II, SPACE-R.	15. NUMBER OF PAGES
	16. PRICE CODE

17. SECURITY CLASSIFICATION OF REPORT Unclassified	18. SECURITY CLASSIFICATION OF THIS PAGE Unclassified	19. SECURITY CLASSIFICATION OF ABSTRACT Unclassified	20. LIMITATION OF ABSTRACT UL